XXI International Congress of the Carpathian Balkan Geological Association (CBGA 2018)
Berichte der Geologischen Bundesanstalt, v. 126, p. 81 – 136

Field Trip Pre-EX-6

Paleogene Events in the sedimentary record of outcrops in Salzburg and eastern Bavaria

HANS EGGER[1], ALFRED UCHMAN[2]

[1] Geological Survey of Austria, Neulinggasse 38, 1030 Vienna, Austria. johann.egger@geologie.ac.at
[2] Institute of Geological Sciences, Jagiellonian University, Kraków, Poland. alfred.uchman@uj.edu.pl

Editorial note

With the exception of Stop 4 and additional information on Stop 1, this guidebook is a short version of the field trip guidebook for the "Climate and Biota of the Early Paleogene" Conference, held in Salzburg in June 2011. Bibliographic reference to this publication: Egger, H. (ed): Climate and Biota of the Early Paleogene, Field-Trip Guidebook, 5-8 June, Salzburg, Austria. Berichte der Geologischen Bundesanstalt. 86, 132pp. This publication can be downloaded from the webpage of the Geological Survey of Austria. The help of Markus Kogler in preparing the figures is gratefully acknowledged.

Introduction

Hans Egger

The Eastern Alps, a 500 km long segment of the Alpine fold-and-thrust belt, originate from the northwestern Tethyan realm. The modern structure of the Eastern Alps is the result of the convergence between the European and the Adriatic Plates (Fig. 1). Separation of these plates started by oblique rifting and spreading in the Permian and Triassic and continued during the Jurassic by the formation of oceanic lithosphere in the Penninic basin. The structural evolution of this basin was linked to the opening of the North Atlantic (e.g. Frisch, 1979; Stampfli et al., 2002). Due to the presence of lower Eocene deep-marine sedimentary rocks in the Penninic units, it is clear that the final closure of the Penninic Ocean did not occur before the Eocene (see Neubauer et al., 2000 for a review).

As a result of the oblique collision of the European and Adriatic plates the elimination of the Penninic Ocean started in the West and prograded continuously to the East. Thrusting in the Eastern Alps started at latest in the Middle Eocene whereas in the adjacent Western Carpathians the onset of thrust formation was around the Eocene-Oligocene boundary (see Decker & Peresson, 1996 for a review). In the Eastern Alps continuing convergence during the Miocene caused lateral tectonic escape of crustal wedges along strike slip faults, which strongly affected the nappe complex of the Eastern Alps. A recent review on the complicated structural development of the Eastern Alps is given by Brückl et al. (2010).

The northern rim of the Eastern Alps consists of detached Jurassic to Paleogene deposits, which tectonically overlie Oligocene to lower Miocene Molasse sediments. From north to south these thrust units originate from (1) the southern shelf of the European Plate (Helvetic nappe complex), (2) the adjacent passive continental margin (Ultrahelvetic nappe complex), (3) the abyssal Penninic Basin (Rhenodanubian nappe complex) and (4) the bathyal slope of the Adriatic Plate (nappe complex of the

Northern Calcareous Alps). Thrusting and wrenching from the Upper Eocene on destroyed the original configuration of these depositional areas and, therefore, the original palinspastic distance between the sedimentary environments of the studied sections is not known. During our field trip, Paleogene sections along a north-south transect within these four nappe complexes will be visited.

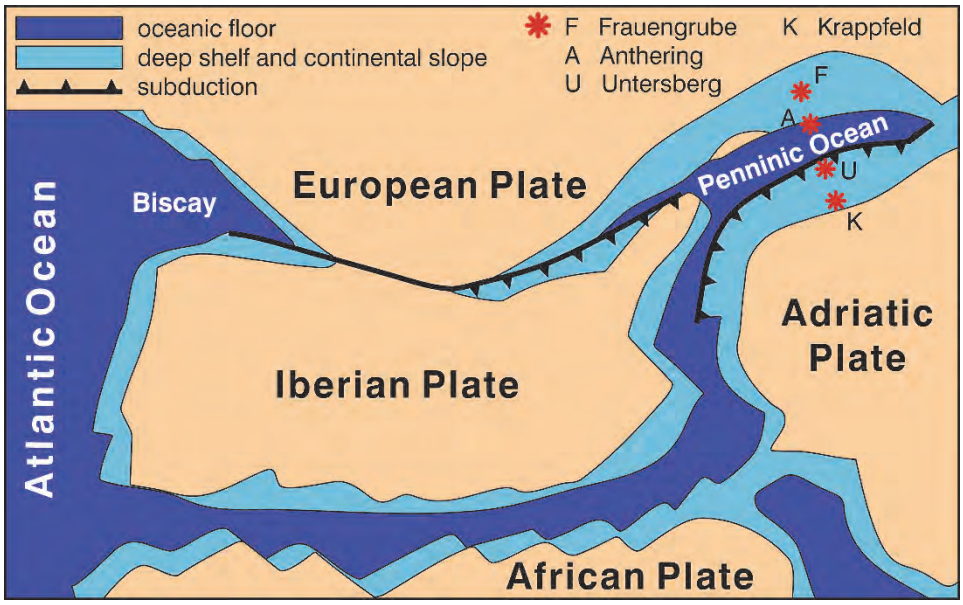

Fig. 1: Schematic paleogeographic map of the NW Tethys and neighbouring areas showing the location of the Alpine environmental areas in the early Paleogene /simplified and modified after Stampfli et al., 1998).

The shallow water sedimentary record of the **Helvetic shelf** is punctuated by a number of stratigraphic gaps, which become more pronounced in direction to the coast of the European continent in the north. So, in the North-Helvetic realm, Paleocene deposits are absent because there the basal Lutetian (calcareous nannoplankton Sub-Zone NP15a) of the Adelholzen beds (STOP 4) with an erosional unconformity overlies the Maastrichtian of the Gerhartsreith Formation (Fig. 3). The Adelholzen Beds (Schafhäutl, 1846) are an equivalent of the Bürgen Formation in Switzerland where an equivalent hiatus between the Cretaceous and the Eocene occurs (Menkveld-Gfellner, 1997). Basinward, this main hiatus is less extended and comprises only the uppermost Paleocene (upper part of Zone NP9) and the lowermost Eocene (Zones NP10 and NP 11 - Egger et al., 2009) in the southern part of the Helvetic shelf (Frauengrube section – STOP 3). A tectonically disturbed but continuous record exists across the K/Pg-boundary of the South-Helvetic domain (Kuhn & Weidich, 1987).

Towards south, the Helvetic shelf gradually passed into the **Ultrahelvetic continental slope**. Depending on the paleodepth at this slope, the pelitic rocks of the Ultrahelvetic unit display varying contents of carbonate. Since Prey (1952), these pelitic deposits were assembled to the informal lithostratigraphic unit Buntmergelserie, which was thought to comprise the Albian to upper Eocene. However, only very few small outcrops of Paleocene to middle Eocene have been recognized and most of them have unclear tectonic positions due to a strong tectonic overprint.

Recently, Egger & Mohamed (2010) recognized a stratigraphic contact between upper Maastrichtian (calcareous nannoplankton Zone CC25) Buntmergelserie and the uppermost Maastrichtian (CC26) to lowermost Eocene (NP11, NP12?) turbidite succession of the Achthal Formation at the Goppling section (STOP 5). This 350 m thick formation is interpreted as the infill of a slope basin, which formed

as a result of block faulting of the continental margin. Deposition took place partly below the planktonic foraminiferal lysocline and partly below the CCD.

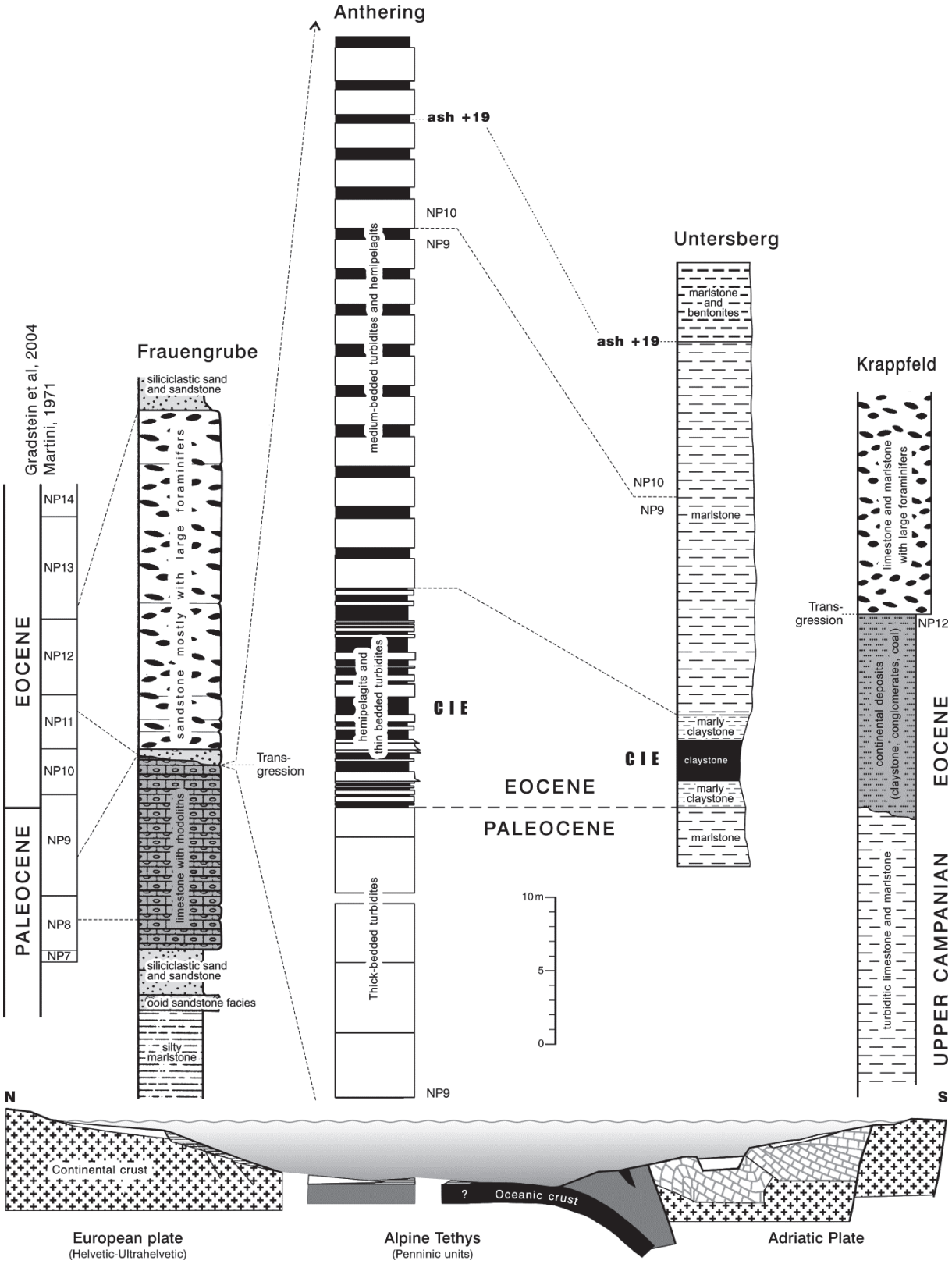

Fig. 2: Correlation and paleogeographic position of Paleogene sections across the Penninic Basin.

Fig. 3: Transgressional contact between the Gerhardtsreit Formation (Maastrichtian) and glauconitic sandstone of the Adelholzen Formation (Lutetian) at the Wimmern section (Bavaria).

Sedimentary successions rich in turbidites other than the Achthal Formation, are known from a number of Ultrahelvetic sites. In Vorarlberg (westernmost Austria), grey turbidites and hemipelagic marlstone (Kehlegg beds) were assigned to the Ultrahelvetic unit by Oberhauser (1991). The base of the Kehlegg beds is situated around the K/Pg-boundary. The unit comprises the entire Paleocene (Egger, unpublished) and its top is tectonically truncated by an overthrust. In a more southerly paleogeographic position on the slope, the deep-water system of the Feuerstätt thrust unit was deposited, exposed in Vorarlberg and southwestern Germany (see Schwerd and Risch, 1983 for a review). There, turbidites and intervening red claystone ("Rote Gschlief-Schichten") of Paleocene and early Eocene age may represent the in-fills of adjacent slope basins at different paleodepths on the continental slope (Weidich and Schwerd, 1987; Schwerd, 1996). Farther to the east, in Lower Austria, Paleocene to Eocene turbidite successions associated with Buntmergelserie are reported by Prey (1957).

In summary, the style of early Paleogene turbidite sedimentation on the European continental margin seen at the Goppling section was not a unique phenomenon. Rather, it occurred at several sites along the strike of the Ultrahelvetic thrust unit in the Eastern Alps. Nevertheless, it is unlikely that these deposits originated from the same basin. Instead, a number of small sub-basins can be assumed, which due to the different subsidence histories and their different bathymetric positions, probably cannot be directly correlated.

The largely synchronous formation of different sub-basins along the strike of the Ultrahelvetic slope points to large-scale tectonic deformation of the continental margin, starting in the late Maastrichtian. The subsidence of intra-slope basins can be related to an extensional tectonic regime. However, for the same period, Nachtmann and Wagner (1987), Wessely (1987), and Ziegler et al. (2002) all document strong intra-plate compressional deformation of the foreland of the Eastern Alps. Together with the data from the Goppling section and other occurrences of the Ultrahelvetic unit, this implies that the southern European plate was simultaneously affected by extension and compression. Here, this style of deformation is typical for anastomosing strike-slip fault zones in convergent settings (e.g. Crowell, 1974).

The well-established contractional deformation event, which affected the European plate in Late Cretaceous times, was explained by two different models. In the first one, strike-slip faulting was driven by the oblique convergence of the European and African plates resulting in a dextral transpressional tectonic regime subsequently to the onset of the collision (Ziegler, 1987). In the second model, this deformation is seen as the result of an important change in relative motion between the European and African plates causing pinching of Europe´s lithosphere between Africa and Baltica (Kley and Voigt, 2008). This model explains better than the collision model the uniform N to NE intraplate shortening of the European plate during the Late Cretaceous event and is also consistent with the NE-SW trending strike-slip faults, which affected the European margin and led to the formation of slope-basins.

Syndepositional faulting and the associated alteration in margin topography, changed sediment dispersal and accumulation not only on the slope but also in the adjacent “Rhenodanubian Flysch” of the **Penninic basin**. There, a dearth of turbidite sedimentation (=Strubach-Tonstein) has been recognized in the Paleocene of the Rhenodanubian Group (Egger, 1995). This was interpreted to be the result tectonic activity that caused a cut-off of the basin from its source areas (Egger et al., 2002). More precisely, the data presented suggest that the above mentioned structurally controlled slope-basins acted as sediment traps and prevented turbidity current by-pass to the main basin.

The Rhenodanubian Flyschzone constitutes an imbricated nappe complex trending parallel to the northern margin of the Eastern Alps. The deep-water sediments of Barremian to Ypresian age were formalized as Rhenodanubian Group (RG) by Egger and Schwerd (2008). The RG consists primarily of siliciclastic and calcareous turbidites but thin, hemipelagic claystone layers occur in all formations of the RG and indicate a deposition below the local calcite compensation depth, probably at palaeodepths >3000 m (Butt, 1981; Hesse, 1975). Paleocurrents and the pattern of sedimentation suggest that the deposition occurred on a flat, elongate, weakly inclined abyssal basin plain (Hesse, 1975, 1982). Compared to other turbidite basins, the depositional area of the Rhenodanubian Group is characterized by low sedimentation rates. An average sedimentation rate for the Cretaceous basin fill, incorporating both turbidites and hemipelagites, of only 25 mm kyr^{-1} has been calculated (Egger & Schwerd, 2008).

Lithostratigraphic classification of the Paleogene deposits of the Rhenodanubian Flysch has been proposed by Egger (1995) who distinguished three distinct lithological units in the area of Salzburg. In the upper Maastrichtian and Danian the Acharting Member of the Altlengbach Formation is characterized by thin- to medium-bedded turbidites, which display base-truncated as well as complete Bouma sequences. Usually the upper part of the Bouma sequences consist of medium-grey clayey marl which represents c. 35 % of this member whereas the percentage of intervening green coloured hemipelagic shale layers is less than 15 %. A distinct feature of this turbidite facies is the intercalation

of thick-bedded and coarse grained sandstones with high amounts of mica and quartz. These are marker beds for mapping the Altlengbach Formation. Calcareous nannoplankton zone NP3 was found in a sequence of very thin-bedded and fine-grained turbidites. Further up-section, hemipelagic claystone (Strubach Tonstein) becomes the dominant rock-type suggesting starvation of turbidite sedimentation. This claystone-rich interval is regarded as part of the Acharting Member.

The lower boundary of the 50 m thick Strubach Tonstein is within Zone NP3. New increased input of turbiditic material started within nannozone NP8 and continued until the upper part of zone NP10. In Zone NP8 and in the lower part of Zone NP9 the facies is very similar to that of the Danian part. In the upper part of zone NP9 graded silty marls of the Anthering Formation become the predominant rock type at the expense of sandstones and siltstones. The base of the Anthering Formation is at the P/E-boundary, which is characterized by the common occurrence of hemipelagic claystone.

The rate of hemipelagic sedimentation in the Paleocene can be calculated using the Strubach Tonstein, which was deposited during a period of about 6 my between calcareous nannoplankton Zones NP3 and NP8. Excluding the turbidites the rate of hemipelagic sedimentation has been calculated as ca. 8 $mmky^{-1}$. Similar values (7 $mmky^{-1}$ resp. 9 $mmky^{-1}$) were assessed for the middle and upper part of Zone NP10, whereas a hemipelagic sedimentation rate of 49 $mmky^{-1}$ has been calculated for the Carbon Isotope Event (CIE)-interval at the Paleocene/Eocene-boundary (Egger et al., 2003). From this it can be summarized that in the Penninic basin the CIE was associated with an increase in the sedimentation rate of siliciclastic hemipelagic material by a factor of six.

In general, the input of terrestrially derived material into the basins increases during episodes of low sea-level as a result of enhanced topographical relief. In the Anthering section, the thickest turbidites of the Thanetian and Ypresian occur in the uppermost 13 m of the Thanetian (Egger et al., 2009). This suggests an episode of massive hinterland erosion, indicating a sea-level drop just prior to the onset of the CIE. This is consistent with data from the Atlantic region (Heilmann-Clausen, 1995; Knox, 1998; Steurbaut et al., 2003; Pujalte and Schmitz, 2006; Schmitz and Pujalte, 2007). The synchroneity of this sea-level drop in the Atlantic and Tethys regions indicates a eustatic fluctuation. Starting with the onset of the CIE, mainly fine-grained suspended material came into the basin and caused a strong increase in hemipelagic sedimentation rates. Such an increase associated with decreasing grain-sizes has been reported from P/E-boundary sections elsewhere and interpreted as an effect of a climate change at the level of the CIE, affecting the hydrological cycle and erosion (Schmitz et al., 2001).

In the lowermost Eocene of the eastern Alps (sub-Zone NP10a) twenty-three layers of altered volcanic ash (bentonites) originating from the North Atlantic Igneous Province have been recorded in lower Eocene deposits (calcareous nannoplankton Sub-Zone NP10a – STOP 2) at Anthering, about 1,900 km away from the source area (Egger et al., 2000). The Austrian bentonites are distal equivalents of the “main ash-phase” in Denmark and the North Sea basin (Fig. 4). The total eruption volume of this series has been calculated as 21,000 km^3, which occurred during 600,000 years (Egger and Brückl, 2006). The most powerful single eruption of this series took place 54.0 million years ago (Ma) and ejected ca. 1,200 km^3 of ash material which makes it one of the largest pyroclastic eruptions in geological history. The clustering of eruptions must have significantly affected the incoming solar radiation in the early Eocene by the continuous production of stratospheric dust and aerosol clouds. This hypothesis is corroborated by oxygen isotope values which indicate a global decrease of sea surface temperatures between 1–2°C during this major phase of explosive volcanism.

Equivalents of these bentonites were found also in the sedimentary record of the northern **Adriatic Plate** within the succession of the Northern Calcareous Alps at Untersberg (STOP 1, Egger et al., 1995) and Gams (Egger et al., 2004). The Cretaceous to Paleogene deposits of the Adriatic Plate lithostratigraphically are formalized as Gosau Group. This group comprises mainly siliciclastic and mixed siliciclastic-carbonate strata deposited after Early Cretaceous thrusting. The Gosau Group of the Northern Calcareous Alps can be divided into two parts – a lower part consisting of terrestrial and shallow-water sediments, including bauxites, coal seams, rudist biostromes, and several key stratigraphic horizons rich in ammonites and inoceramids (Lower Gosau Subgroup, Turonian to lower Campanian), and an upper part, comprising deep-water marlstone, mudstone and turbidites (Upper Gosau Subgroup, upper Campanian to Pribonian). Deposition of the Gosau Group was the result of transtension, followed by rapid subsidence into deep-water environments due to subduction and tectonic erosion at the front of the Adriatic Plate (Wagreich, 1993).

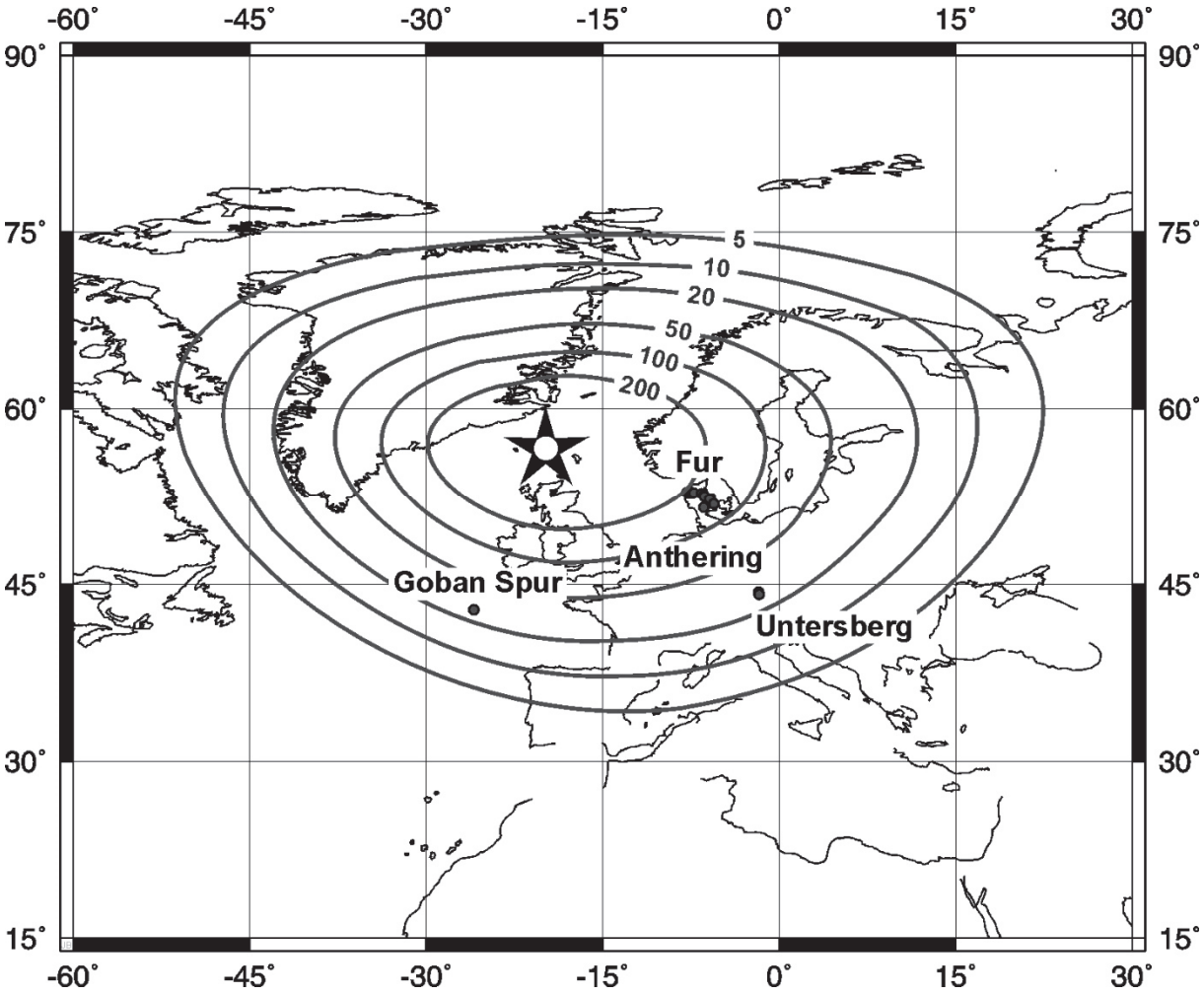

Fig. 4: Map showing the plate tectonic situation at 54 Ma (rotated present day shore lines), the rotated locations where layer +19 was found (solid spheres and locality names), and elliptical isopachs of layer +19 (grey contours, tephra thicknesses in mm) with assumed NAIP-source (star) at one focus.

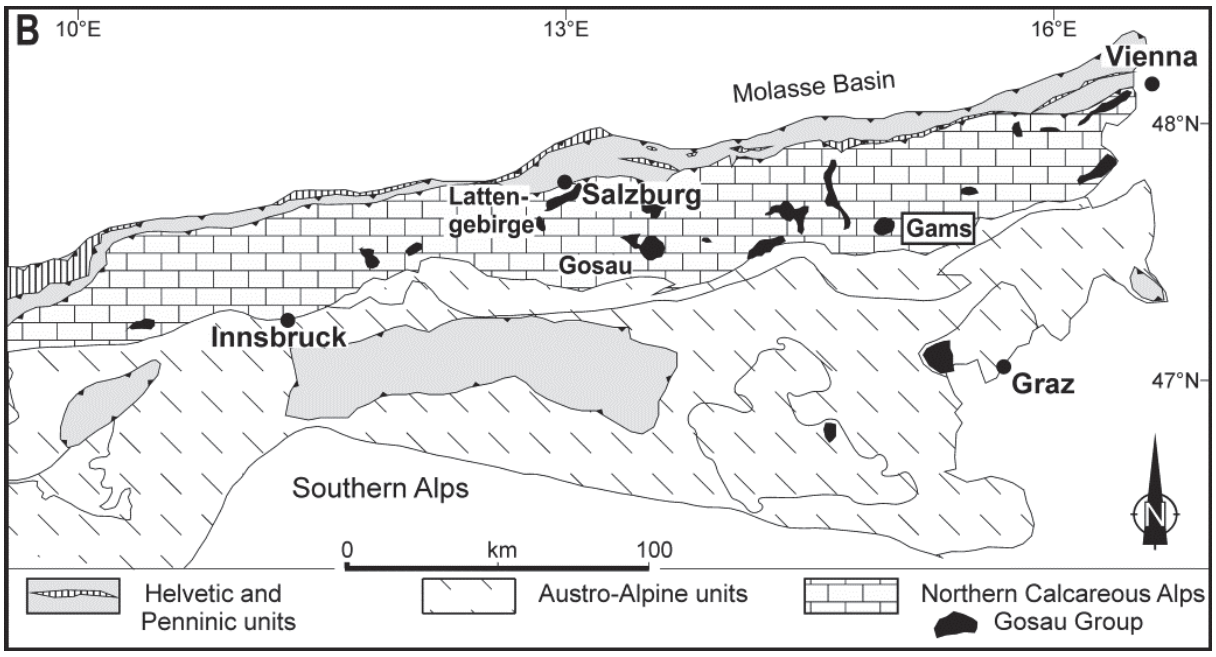

Fig. 5: Location of Gosau deposits in the Eastern Alps.

The Cretaceous/Paleogene-boundary has been studied in five sections of the Nierental Formation of the Upper Gosau Subgroup of the Northern Calcareous Alps (Fig. 5). The first K/Pg boundary in the region was discovered in the *Wasserfallgraben section* of the Lattengebirge in Bavaria (Herm et al. 1981). Perch-Nielsen et al. (1982) reported on biostratigraphical and geochemical results, and Graup and Spettel (1989) measured bulk Ir contents of 4-5 ppb in the boundary clay from this section. The second K/Pg boundary site was identified in the *Elendgraben section* near the village of Gosau in Salzburg (Preisinger et al. 1986; Stradner et al. 1987). The boundary is marked by a 2-4 mm thick yellowish clay layer, which contains up to 14.5 ppb iridium. The third K/Pg boundary site was recognized in the *Knappengraben section* at Gams (Stradner et al. 1987). Again, the boundary clay is of light yellow color and contains up to 7 pbb iridium. Lahodynsky (1988) studied the lithology of the Knappengraben and Elendgraben sections and interpreted their sedimentological and geochemical features as the result of extensive volcanic eruptions. Recently, Grachev et al. (2005, 2007, 2008) followed this interpretation. The fourth K/Pg boundary site has been described at the *Rotwandgraben section* also near the village of Gosau, about 2.5 km to the southeast of the Elendgraben section (Peryt et al. 1993, 1997). The maximum Ir content in the boundary clay has been determined to be 7 ppb.

In the Northern Calcareous Alps, Paleocene/Eocene (P/E)-boundary sections were studied at Untersberg near Salzburg (Egger et al., 2005) and Gams in Styria (Egger et al., 2009; Wagreich et al., 2011). At the Untersberg section the P/E-boundary is characterized by grey and red claystone intercalated into the dominating marlstone of the succession. At its top, the claystone displays a gradual increase in calcium carbonate contents. This transition zone from the red claystone to the overlying grey marlstone indicates a deposition within the lysocline. The gradual change of carbonate content within the transition zones suggests a slow shift of the level of the lysocline and CCD at the end of the CIE and has been described also from other sections (e.g. Zachos et al., 2005).

Like on the Helvetic shelf in the north of the Penninic basin (see above), a major stratigraphic gap exists in the sedimentary record of the **shelf of the Adriatic plate** at the southern rim of the basin. Lower Eocene deposits rest with an erosional unconformity on Upper Campanian marlstone of the *Tranolithus phacelosus* Zone (Sub-Zone CC23a). In the Pemberger quarry (unfortunately, this outcrop

was destroyed in 2011), from the base of the marine deposits *Assilina placentula, Nummulites burdigalensis kuepperi, Nummulites increscens,* and *Nummulites bearnensis* were described (Schaub, 1981; Hillebrandt, 1993). This fauna is indicative of the lower part of shallow benthic zone SBZ10, which has been correlated with calcareous nannoplankon zone NP12 (Serra-Kiel et al., 1998).

Due to their similar stratigraphic positions, Egger et al. (2009) assumed that the Ypresian transgressions at the shelves of the European and Adriatic Plates originated from the same eustatic event, which was the highstand of the TA2 supercycle in the global sea-level curve (Haq et al., 1987). At the Adriatic Plate, at the base of the marine transgression, black shales occur containing a rich and well preserved tropical palynoflora, indicating *Nypa*-dominated mangrove type forests, which reflect the early Eocene climate optimum (Hofmann et al., 2011). The onset of this episode of tropical climate was near the top of magnetic Chron 24, which coincides with the NP11/NP12 zonal boundary (Collinson, 2000; Gradstein et al., 2004).

The youngest deposits of the Gosau Group at Krappfeld are of Lutetian age. Hillebrandt (1993) reported both *Nummulites hilarionis* and *Nummulites boussaci*, which indicate shallow benthic zone SBZ14, and *Nummulites millecaput*, which is indicative for shallow benthic zone SBZ15. These foraminiferal zones can be correlated with the upper part of calcareous nannoplankton Zone NP15 and the lower part of Zone NP16 (Serra-Kiel et al., 1998).

Stop 1 Untersberg Section near Fürstenbrunn

Hans Egger, Alfred Uchman
Topic: Paleocene/Eocene-boundary and lower Eocene bentonites section in bathyal marlstone and claystone
Tectonic unit: Northern Calcareous Alps (Adriatic Plate)
Lithostratigraphic unit: Gosau Group, Nierental Formation
Chronostratigraphic units: Upper Paleocene to Lower Eocene
Biostratigraphy: Calcareous Nannoplankton Zones NP9 and NP10a; Planktonic Foraminifera Zones P5 to E3
Location: Tributary of the Kühlbach near Fürstenbrunn (Fig. 6B)
Coordinates: 47° 44´ 19“ N, 012° 59´ 04“ E
References: Egger et al. (2005), Egger & Brückl (2006), Hillebrandt (1962), Hagn (1981)

Stop 1a: Paleocene/Eocene-boundary

From the bus stop it is a 10 minute downhill walk through the forest (no trail!) to reach the outcrops, which are located along the course of a creek. Estimated duration of the stop is 1.5 hours.

The Paleogene deposits of the Untersberg region were examined by von Hillebrandt (1962 and in Hagn, 1982. The more than 1000 m thick Paleogene succession of the Untersberg area consists predominantly of marlstone displaying carbonate contents between 40wt% and 50wt%. Abundant planktonic foraminifera and calcareous nannoplankton are the main source of the carbonate. Von Hillebrandt (1962) already recognized the importance of the benthic foraminiferal extinction at the end of the Paleocene and Egger et al. (2005) re-examined this outcrop. However, at that time the exposure was worse and only part of the CIE-interval was outcropping. In 2010, a flood event due to torrential rain significantly improved the outcrop situation and revealed also minor faults along the dipping planes.

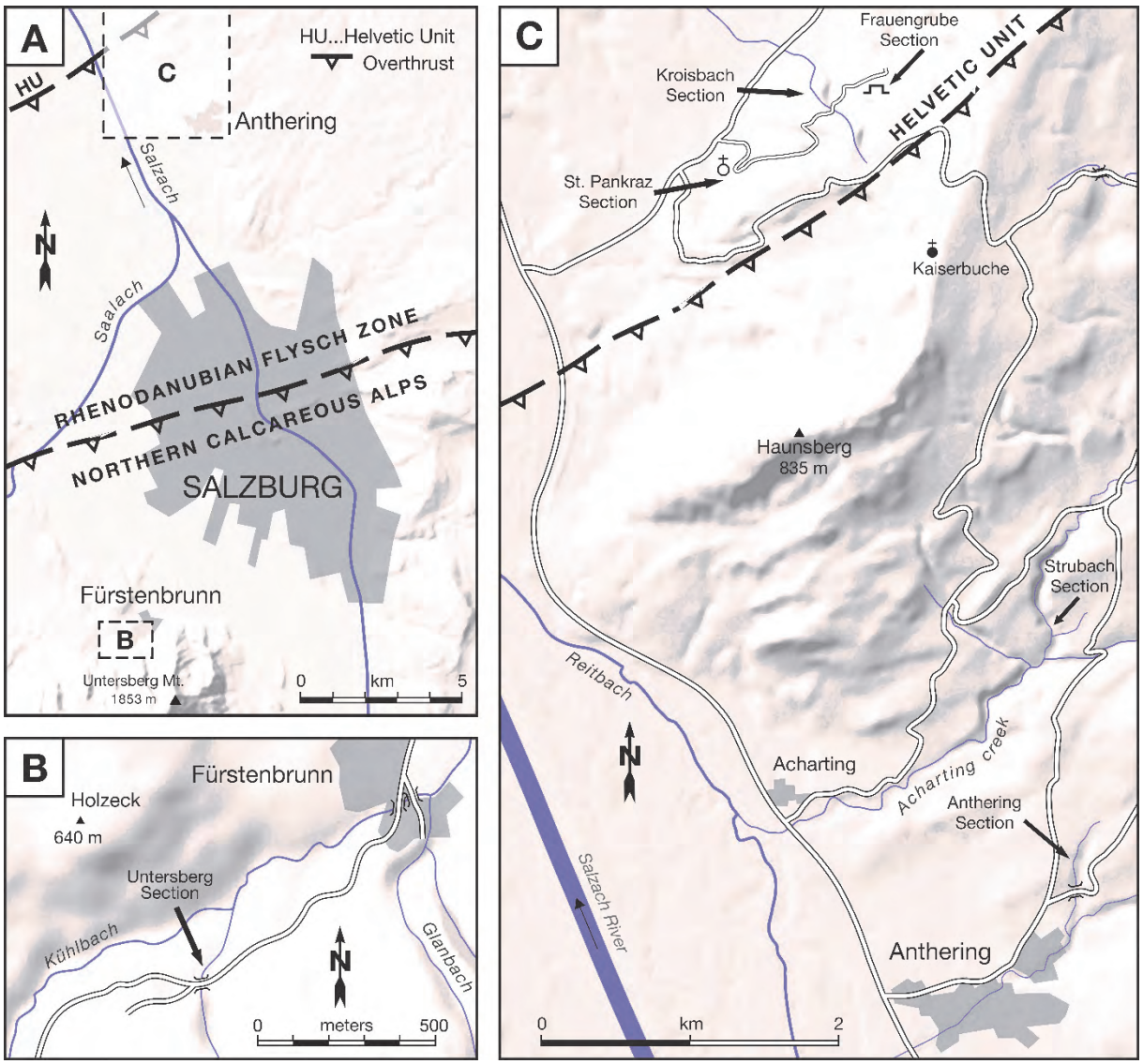

Fig. 6: Route map for outcrops 1 – 3 of the field trip.

Fig. 7: Photograph of the outcrop 1a at Untersberg showing the CIE-interval.

At the base of the new outcrop (Fig. 7) grey marlstone shows a sharp contact to grey claystone, which is overlain by red claystone. The claystone at the P/E-boundary indicates a deposition below the CCD. Excluding the carbonate content, the mean percentages of the siliciclastic components are almost identical below and above the CIE-interval: 16.3% quartz and feldspar and 83.7% clay minerals from the interval above the CIE and 16.6% quartz and feldspar and 83.4% clayminerals below the CIE. However, within the CIE-interval the mean percentage of quartz and feldspar is 24.8%, which is equivalent to an increase of 49% in relation to the other parts of the section.

The clay mineral assemblage at Untersberg is strongly dominated by smectite (72wt%), followed by illite (18wt%), kaolinite (6wt%) and chlorite (4wt%) (Fig. 8). The abundance of smectite throughout the studied section, together with the absence of mixed-layers, indicates that the rocks of the Untersberg section were not affected by deep-burial diagenesis. Consequently, diagenetic effects on the composition of clay mineral assemblages can be ruled out.

At its top, this claystone displays a gradual increase in calcium carbonate contents (Fig. 9) already documented by Egger et al. (2005). This transition zone to the overlying grey marlstone indicates a deposition within the lysocline, which is the water depth where carbonate dissolution rates are greatly accelerated (Berger, 1970). The gradual change of carbonate content within the transition zones suggests a slow shift of the level of the lysocline and CCD at the end of the CIE and has been described also from sections elsewhere (Zachos et al., 2005).

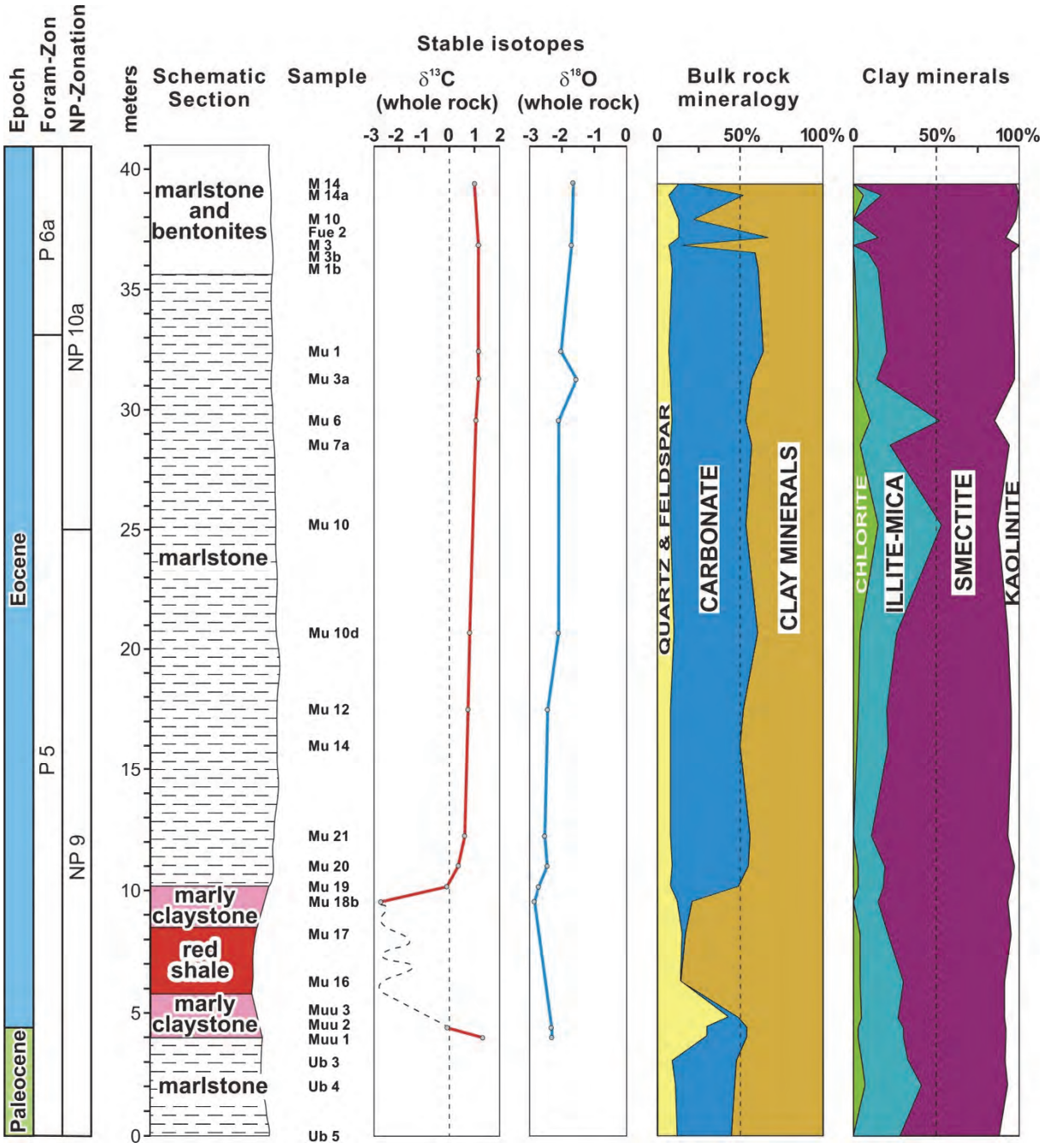

Fig. 8: Carbon isotope values, bulk rock mineralogy, and composition of clay mineral assemblages across the Paleocene–Eocene boundary.

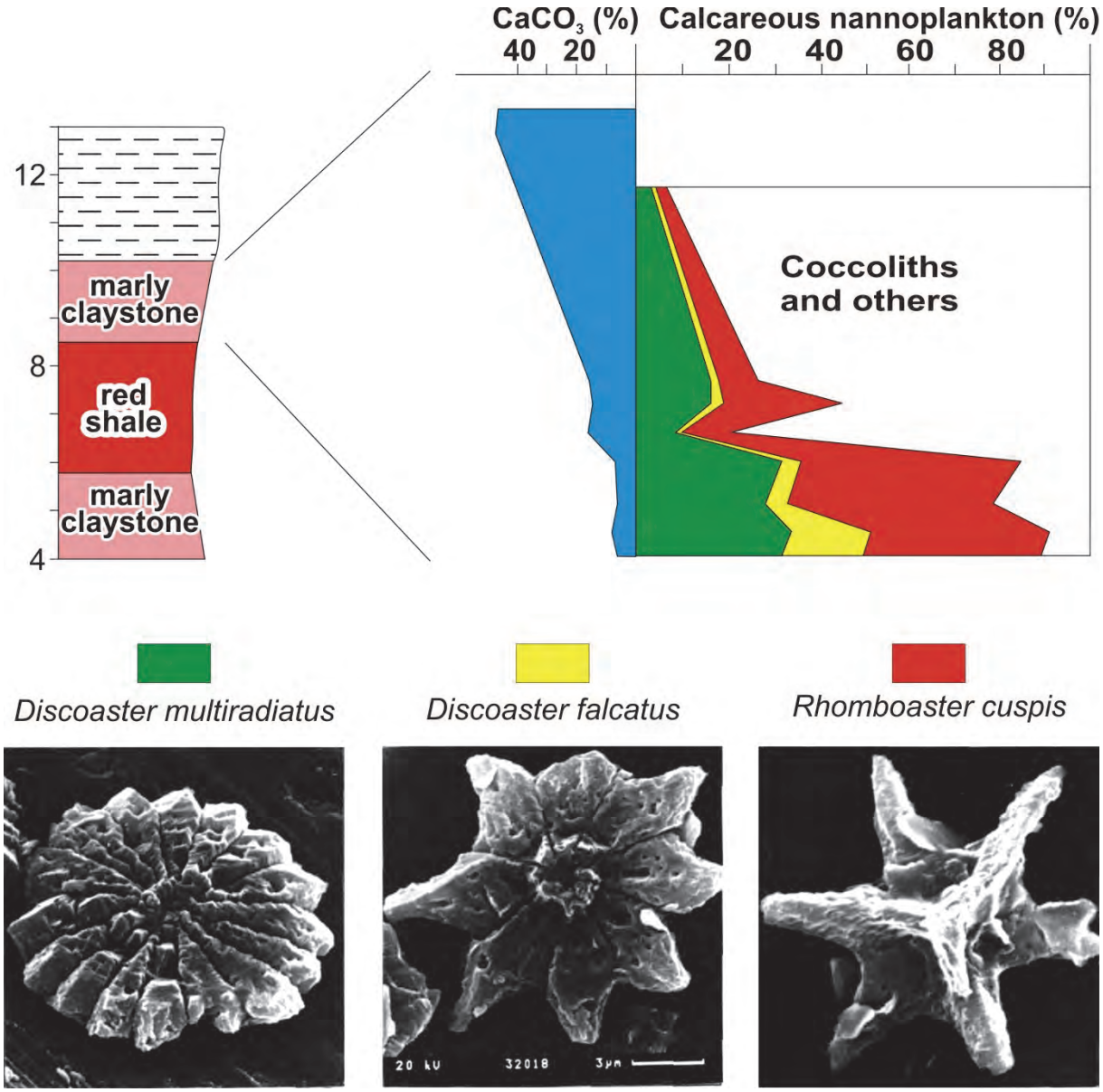

Fig. 9: Percentages of Discoaster multiradiatus, Discoaster falcatus, and Rhomboaster cuspis in the calcareous nannoplankton assemblages and calcium carbonate percentages at the top of the CIE–interval (scale bar represents 3 µm for all photographs).

Calcareous nannoplankton

Calcareous nannofossils were found in the marlstone and in the transition zones (marly claystone) between the marlstone and the shale. They are abundant (> 30 specimens per field of view) in the samples from the marlstone, whereas their abundance is low (< 10 specimens per field of view) in the samples from the transition zones. The preservation of nannofossils is moderate in the marlstone and poor in the transition zone according to the classification of Steinmetz (1979). In the moderately preserved samples the majority of the specimens are slightly etched but all taxa can be easily identified and diversity is about 16 species per sample on average. In the poorly preserved samples, the majority of specimens are deeply etched, identification of taxa is difficult and the diversity is only about 6 species per sample.

Reworked specimens are present in the marlstone samples, with rare Cretaceous species appearing (less than 1% of the nannofossil assemblage). Reworking has affected mainly Upper Cretaceous deposits, indicated by the occurrences of *Micula decussata, Prediscosphaera cretacea, Lucianorhabdus cayeuxii, Broinsonia parca, Ceratolithoides aculeus, Uniplanarius trifidus* and *Arkhangelskiella cymbiformis*. In one sample (M3b) typical Lower Cretaceous species (*Micrantolithus hoschulzii* and *Nannoconus steinmannii*) were also found. However, the relatively common *Watznaueria barnesae* specimens in most samples may in part also originate from Lower Cretaceous deposits, as this species is abundant throughout the entire Cretaceous.

The Paleogene nannoflora is dominated by *Coccolithus pelagicus*, which usually accounts for about 90% of the nannoplankton assemblages, with the exception of the poorly preserved assemblages of the CIE-interval. *Discoaster multiradiatus*, the index species of Zone NP9, is another common species and occurs in all samples. Species of the stratigraphically important genus *Fasciculithus* are rare in the Untersberg section, except in the samples from below the CIE. *Scapholithus apertus* is the only species which becomes extinct at the Palaeocene-Eocene boundary of the Untersberg section.

The first specimens of the genus *Rhomboaster* occur just below the base of the CIE. There, short-armed specimens of *Rhomboaster cuspis* are exceedingly rare. In contrast, in the samples from the top of the CIE-interval *Rhomboaster cuspis* is the dominant species (up to 49% of the assemblages) followed by *Discoaster multiradiatus* and *Discoaster falcatus* and *Discoaster araneus*. In other Tethyan sections *Discoaster anartios* (Bybell and Self-Trail, 1994) co-occurs with *Discoaster araneus*; however, this species has not been found at Untersberg. Coccoliths are absent or extremely rare in this CIE-assemblage.

The unusual composition of the nannoplankton assemblage of the marly claystone at the top of the CIE-interval is an effect of carbonate dissolution because, synchronously with increasing carbonate content, the calcareous nannoplankton shows better preservation and a higher diversity (Fig. 9). The species diversity in nannoplankton assemblages is, to large extent, controlled by selective dissolution of skeletal elements. Bukry (1971) recognized that *Discoaster* is the most dissolution-resistant genus among the Cenozoic genera, followed by the genus *Coccolithus*. At Untersberg, the high percentages of *Rhomboaster* in the transition zone assemblages are most probably an effect of selective dissolution, indicating that *Rhomboaster* has a similar resistance to dissolution as *Discoaster*.

Foraminifera

Planktonic and benthic foraminifera are very abundant in most of the studied samples, although, as a result of carbonate dissolution, their preservation is poor across the CIE-interval. There, the assemblages are strongly dominated by agglutinating taxa. A specific determination was often difficult to make as many planktonic foraminifera specimens are corroded or deformed. For this reason no quantitative analysis of the foraminifera fauna was conducted, despite recording 191 different taxa in 19 samples, excluding species reworked from the Upper Cretaceous and Lower Paleocene (mainly Danian). The planktonic foraminiferal biozonation follows the criteria of Berggren and Pearson (2005).

Zone P5 (*Morozovella velascoensis* Partial-range Zone), the uppermost zone in the Paleocene, is defined by the highest occurrence (HO) of *Globanomalina pseudomenardii* and the lowest occurrence (LO) of Acarinina sibaiyaensis. At Untersberg, only reworked specimens of *G. pseudomenardii* occur, wheras *A. sibaiyaensis* is absent and has not been found in Eastern Alpine sections till now. The assignment of the lowermost part of the studied section to Zone P5 is due to the occurrence of

Morozovella subbotinae, which has a stratigraphic range from Zone P5 to Zone E5. In this part of the section also *M. aequa* and *M. gracilis* occur.

Due to the scarcity of planktonic foraminifera in the claystone of the CIE-interval no zonal attribution was possible. In the overlying marlstone (sample MU 19/97) *Pseudohastigerina wilcoxensis* was found, indicating Zone E2 (*Pseudohastigerina wilcoxensis/Morozovella velascoensis* Concurrent-range Zone). This zone is defined as the interval between the lower occurrence (LO) of *P. wilcoxensis* and the highest occurrence (HO) of *M. velascoensis*.

M. velascoensis has its HO in sample MU 10d/97. Further up-section, rare specimens of this species (sample MU 6/97) are considered to be reworked. The LO of *Morozovella edgari* is used to assign the highest part of the section to Zone E3 (*Morozovella marginodentata* Partial-range Zone). This zone is defined by the HO of *M. velascoensis* and the LO of *M. formosa*, however, the latter species does not occur in our samples

The distribution of calcareous benthic foraminifera is similar to those of other deep-water sections (see Thomas, 1998, for a review). *Gavelinella* cf. *beccariiformis* has its HO at the onset of the CIE. The post-extinction calcareous benthic foraminifera assemblages are dominated by *Nuttalides truempyii* (very small specimens), *Abyssamina poagi, Anomalinoides nobilis, A. praeacutus, Oridorsalis spp*. and a number of pleurostomellids (e.g. *Ellipsoglandulina, Ellipsoidella, Ellipsopolymorphina, Nodosarella, Pleurostomella*). This assemblage is typical of lower bathyal to abyssal environments (van Morkhoven et al., 1986). For example, *Abyssamina poagi* occurs between 1700 m and 4000 m depth, and *Oridorsalis lotus* indicates a depth of between 800 m and 1900 m. This suggests a palaeodepth of about 2000 m (lower bathyal) for the deposition of Untersberg section.

The agglutinating foraminiferal fauna consists of 68 species, 25 of which (37% of the entire fauna) occur exclusively at the base of the succession and end within the CIE-interval. These species are *Ammodiscus cretaceus, Aschemocella carpathica, A. grandis, Bathysiphon? annulatus, Caudammina arenacea, C. excelsa, C. ovulum, Dorothia beloides, Glomospira diffundens, G. glomerata, G. serpens, Haplophragmoides walteri, Hormosinella distans, Hyperammina lineariformis, Karrerulina horrida, Psammotodendron? gvidoensis, Psammosiphonella* sp., *Remesella varians, Rzehakina fissistomata, Saccamina grzybowskii, Silicobathysiphon* sp., *Subrheophax pseudoscalaris, S. splendidus, Trochamminoides folius*, and *T. subcoronatus*. In the upper part of the succession the typical assemblage with *Paratrochamminoides* and *Trochamminoides* has disappeared, but *Recurvoides gerochi* and *R. pseudoregularis* are still common. Within the CIE-interval the agglutinated assemblage is dominated by *Glomospira* spp. Such assemblages, similar to the „Biofacies B“ assemblage or to the „*Glomospira* event“ occur in the Cretaceous and in the Early Eocene of the North Atlantic and Tethys (comp. Kuhnt et al., 1989; Kaminski et al., 1996).

Radiolarians

Occurrences of radiolarians are restricted to the lower part of the section, where they are abundant from samples Mu18a to Mu14 and common in samples Muu2, Mu10, and Mu10d. In the finest grained sieve-residue of sample Mu19, radiolarians are the dominant component. The radiolarians are all spheroidal spumellarians, but are taxonomically indeterminable, since their siliceous skeletons are poorly preserved, due to their replacement by smectite. The abundance of siliceous plankton indicates high nutrient levels in oceanic surface waters in the basal Eocene. A coeval increase in both sedimentation rates and the amounts of terrestrially derived quartz and feldspar suggests that this

high primary productivity was the result of enhanced continental run-off. No radiolarians were found further up-section in outcrop 1b.

Trace fossils

The trace fossil assemblage is low diverse and consists only of four ichnotaxa: *Chondrites* isp., *Planolites* isp., *Thalassinoides* isp., and *Zoophycos* isp. They are mostly visible in cross section what precludes determinations at the ichnospecies level.

The trace fossil distribution pattern of the studied section shows a clear three-fold subdivision.The highest abundance and diversity of trace fossils was recognized in the lower part of the section (0 - 2.40 m), where *Chondrites* isp., *Planolites* isp., *Thalassinoides* isp., *Zoophycos* isp., and large unidentified burrows occur. All ichnotaxa show a more or less continuous record, with the exception of *Zoophycos* and the undeterminable large burrows, which are restricted to a few horizons. Disrupted primary lamination is locally recognized but the major part consists of grey and greenish grey mudstone with occasional red coloured spots and layers.

The middle part of the section (2.40–4 m) is characterized by the presence of primary lamination in a more or less continuous 1.5 m-thick interval, with only very scarce trace fossils. This interval mainly consists of non-calcareous red mudstones, locally with green spots and laminae. Around 3.1 m from the base, primary lamination is undisturbed, while in the remaining part of the interval the primary lamination is disrupted.

The upper part of the section shows less abundant and less diverse trace fossil assemblage than the lower part. *Chondrites* shows a more or less continuous record, and *Thalassinoides* is common, while *Planolites* occurs only sporadically, and *Zoophycos* is absent. One thin layer displays primary lamination.

The trace fossil assemblage is typical of the *Zoophycos* ichnofacies, which is depauperated in some section segments. The *Zoophycos* ichnofacies in Palaoegene is typical for lower bathyal-abyssal depths and low-energy fine-grained facies.

The study of bioturbational structures suggests a temporarily complete extinction of the macrobenthic community during the Paleocene-Eocene transition. Similar observations were made by Nicolo et al. (2010) in the South Pacific and Rodriguez-Tovar et al. (2011) at the Zumaia section at the Bay of Biscay. Both publications explain the severe crisis of benthic communities as a result of oxygen depleted bottom waters. However, the P/E-boundary at the Untersberg and Zumaia sections manifests as a red claystone horizon deposited in an oxic environment. Several factors can be invoked to explain this situation. Extreme oligotrophy on the sea floor can be considered when temperature of deep waters increased by at least few degrees during Paleocene-Eocene transition (e.g. Bowen et al., 2006). The waters can be dense and saline (Braas et al., 1982). Moreover, methane which was released from methane clathrates after the increase in temperature (see Dickens, 2000) might saturate the pore waters and prevent burrowing by macroorganisms. It is an open question, if one of these factors or their combination stopped bioturbation.

Stop 1b: Volcanic ash-layers in the Lower Eocene

Hans Egger

Within grey marlstone (calcareous nannoplankton sub-Zone NP10a; planktonic foraminifera Zone E3) thirteen light yellowish layers consisting essentially of smectite were found. These 0.2 cm to 3 cm thick bentonite layers are interpreted as volcanic ashes. No bentonites were found in either the lower part of zone NP9 or in the overlying sub-zone NP10b, which are exposed in other outcrops of the area. The occurrence of bentonites is therefore exclusively restricted to sub-zone NP10a.

Due to their complete conversion to smectitic clay the original chemical composition of the bentonites must have strongly changed. Consequently, only the immobile elements have been used to assess the composition of the original magma (Winchester and Floyd, 1977). The immobile element contents of most of these altered ash layers show very little variation: Nb 28.3 ± 4.7 ppm, Zr 259 ± 104 ppm, Y 25.0 ± 9.5 ppm, and TiO2 4.82 ± 0.7 wt.% (see Fig. 10).

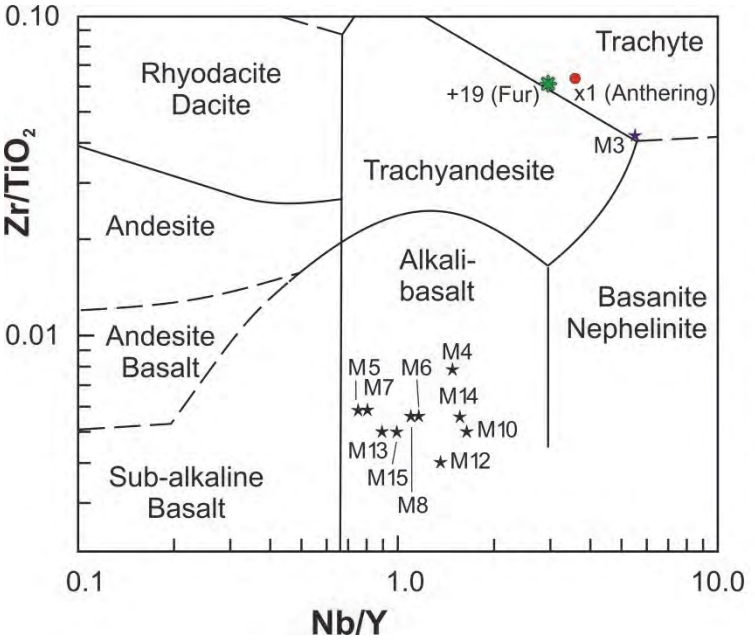

sample	Nb	Zr	Y	TiO_2
M15	28.1	232.8	28.1	47650
M14	33.0	276.9	26.5	51480
M13	28.2	241.6	31.4	49160
M12	26.5	221.4	17.0	54700
M10	31.5	269.9	17.8	55170
M8	25.8	231.8	22.2	43300
M7	24.6	239.1	30.6	42000
M6	28.0	237.8	23.9	44140
M5	25.3	242.5	34.5	42700
M4	31.3	363.0	21.1	46600
M3	121.8	480.6	21.3	11760

All data in ppm.

Fig. 10: Magma composition of different ash-layers by means of immobile element distribution (after Winchester and Floyd, 1977). For comparison, sample +19 from the Danish Fur Formation and sample X1, from the Austrian Anthering Formation, are plotted (from Egger et al., 2000).

These samples plot in the discrimination diagram of different magma sequences in the field of alkali-basalts. Basaltic ashes are rare in the geological record as the generation of basaltic pyroclastics requires an interaction between basaltic lavas and meteoritic water (see Heister et al., 2001, for a review). Layer M3 (Figure 10 has a totally different composition with highly enriched Nb and Zr, equal Y, and depleted TiO2 compared to the other bentonites. It is the oldest and thickest layer of the ash-series and plots at the border of trachyte and trachy-andesite.

The biostratigraphical and geochemical correspondence of these tephras with ashes from the North Sea Basin suggests that these pyroclastic deposits are related to the continental breakup of Europe and Greenland (Egger et al, 2000; Huber et al., 2003; Egger & Brückl, 2006). There, the North Atlantic Igneous Province (NAIP), which is one of the largest basaltic lava accumulations on Earth, formed in the early Paleogene (62–53 Ma), prior to and during the continental break-up between Europe and Greenland (Eldholm & Grue, 1994; Ritchie & Hitchen, 1996; Ross et al., 2005). Beside voluminous flood

basalts and associated igneous intrusions, it produced widespread pyroclastic deposits. From the early Eocene Fur Formation in Denmark more than 200 ash-layers of predominantly basaltic composition have been recorded from this explosive volcanic activity (Knox & Morton 1988; Heister et al. 2001). A numbering system for most of these layers was introduced by Bøggild (1918) and is still in use: The upper, closely spaced layers constitute the "positive series", with layers numbered +1 to +140 in ascending order. The lower, more widely spaced and generally thinner layers make up the "negative series", and are numbered -1 to -39 in descending order.

The paroxysm of this volcanic activity, the positive ash–series, consists of tholeiitic ferrobasaltic layers with the exception of layer +19. In the immobile element diagram of Floyd and Winchester (1976) this layer plots at the border between trachyte and trachyandesite, whereas more detailed geochemical investigations indicate a rhyolitic composition of the original magma (Huber et al., 2003; Larsen et al. 2003). Some of the ashes of the positive series have also been found at many other sites in Denmark, the North Sea, England, the Goban Spur southwest of Ireland, and the Bay of Biscay (Knox, 1984). Based on detailed multi-stratigraphic and geochemical investigations, the most distal equivalents of layer +19 and 22 other layers have been identified in the Anthering and Untersberg outcrops of the Austrian Alps near Salzburg (Egger et al. 2000 and 2005; Huber et al. 2003).

It can be assumed that the ash-layers of the NAIP form important correlation horizons for lower Eocene deposits in large areas of Europe. In addition to the Austrian outcrops, reports of lower Eocene basaltic ash layers exist from Switzerland and Poland (Winkler et al. 1985; Waśkowska-Oliwa & Leśniak 2002), although stratigraphic and geochemical information from these deposits is insufficient for a detailed correlation.

Stop 2 Anthering Section

Hans Egger

Topics: Paleocene/Eocene-boundary section in a succession of deep-water turbidites and hemipelagites
Tectonic unit: Rhenodanubian Flysch Zone (Penninic Basin)
Lithostratigraphic unit: Rhenodanubian Group, Anthering Formation
Chronostratigraphic units: Upper Paleocene to Lower Eocene
Biostratigraphy: Upper part of calcareous nannoplankton Zone NP9 to upper part of Zone NP10
Location: Outcrops of the Kohlbachgraben near Anthering (Figs. 6C, 11)
Coordinates: 47° 53´ 19" N, 013° 01´ 17" E
References: Heilmann-Clausen & Egger (1997), Egger, Heilmann-Clausen & Schmitz (2000), Crouch et al. (2001), Egger et al. (2003), Egger & Brückl (2006), Iakovleva & Heilmann-Clausen (2007), Egger et al. (2009).

From the carpark at the Reinthal inn it is an approx. 10 minutes walk on a small road to the first outcrop of the section, which is located along the course of the Kohlbach creek (no trail!). We examine the section (Fig. 11) walking up-stream from the lower Eocene (NP10) to the uppermost Paleocene (NP9).

The Anthering section is located about 18 km to the north of the Untersberg section as the Anthering and Untersberg sections are separated by the thrust between the Northern Calcareous Alps and the Rhenodanubian Flysch zone, the original palinspastic distance between them must have been much greater than at present. However, reliable data on this distance are lacking.

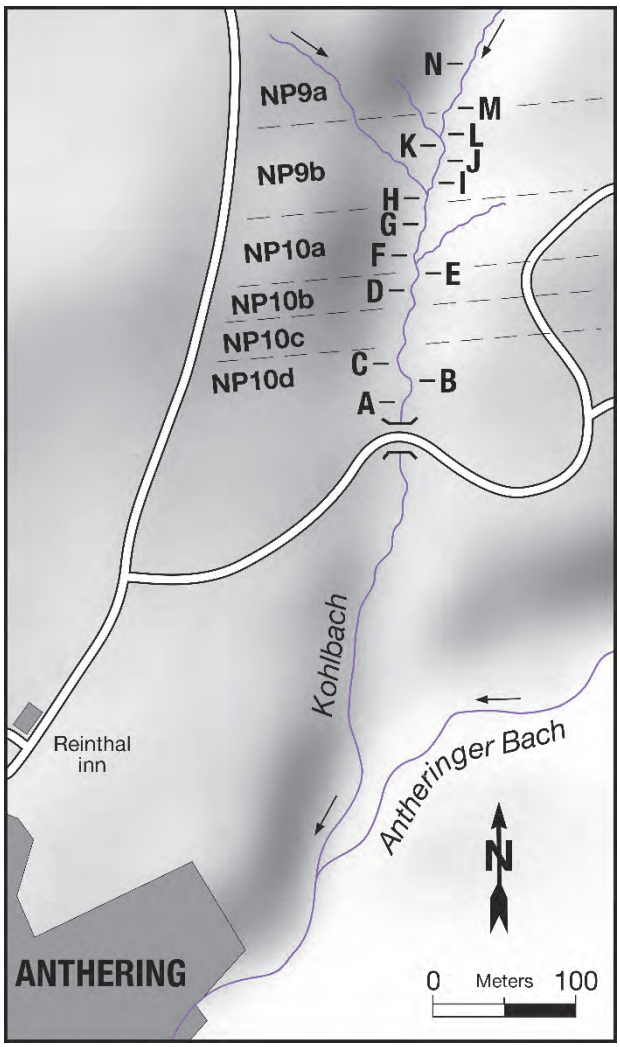

Fig. 11: Location of outcrops and biostratigraphy of the Anthering section.

The 250 m thick upper Paleocene to lower Eocene deposits of the Anthering section, spanning calcareous nannoplankton Zones NP9 and NP10. These sediments comprise the youngest part of the Rhenodanubian Group. This group was deposited on the continental rise to the south of the European plate, which was the main source for the siliciclastic detritus entering the basin. The section is composed of calcareous mud-turbidites with intervening hemipelagic claystone indicating a deposition below the calcite compensation depth. The general sedimentary record of the Anthering-section is typical for an abyssal plain facies. Paleo-water depth estimations by Butt (1981), using foraminifera assemblages, range between 3000 to 5000 m.

In the Eocene part (Anthering Formation) of the section, the turbidite succession is characterized by the predominance of graded silty marlstone, which form about 85% of the succession (Anthering Formation). Occasionally, these turbiditic marlstone layers overlie silty to sandy beds deposited from the same turbidity current. The turbidites usually display base-truncated Bouma-sequences. Turbidites displaying complete Bouma-sequences are very rare. Single turbidite layers can reach thicknesses up to 2 m. The finegrained sand-fraction represents, on average, 5% of the sedimentary rocks and exceptionally up to 10%. The fine-grained (silty-clayey) sediment displays carbonate contents of 29% to 53%. The clay fraction is dominated by smectite.

Fig. 12: Photograph showing outcrop B.

Fig. 13: Flute casts at outcrop B.

Common intercalations of hemipelagic claystone occur between the individual mud-turbidite beds (Fig. 12, 14). The hemipelagic claystones prove a position of the basin-floor below the local calcite compensation depth. They are devoid of carbonate and display sharp contacts to the turbiditic marls. Usually the claystones show a greenish to greyish colour (0.15wt% organic carbon on average) with a large number of dark spots as indications of intensive bioturbation. Only in the middle part of the section (outcrop E and one layer in outcrop D) darkgrey homogeneous claystones with abundant pyrite framboids and relatively high contents of organic carbon (0,94wt% on average) occur (Fig. 15). These black shales indicate an oxygen deficient environment at the basin floor. As they occur together with bentonite layers, volcanism might have led to eutrophic conditions and high plankton productivity responsible for the anoxic conditions.

In the lowermost Eocene (Subzone NP10a) at the Anthering section, 23 layers of altered volcanic ash (bentonites) originating from the North Atlantic Igneous Province have been recorded, about 1,900 km away from the source area (Egger et al., 2000). The Austrian bentonites are between 1mm and 30 mm thick and are considered to be distal equivalents of the “main ash-phase” in Denmark and the North Sea basin. Egger & Brückl (2006) have calculated the total eruption volume of this series as 21,000 km^3, which occurred in 600,000 years. The most powerful single eruption of this series took place 54.0 million years ago (Ma) and ejected ca. 1,200 km^3 of ash material which makes it one of the largest pyroclastic eruptions in geological history. The clustering of eruptions must have significantly affected the incoming solar radiation in the early Eocene by the continuous production of stratospheric dust and aerosol clouds. This hypothesis is corroborated by oxygen isotope values which indicate a global decrease of sea surface temperatures between 1–2°C during this major phase of explosive volcanism.

The Anthering section displays the global negative carbon isotope excursion (CIE) and the acme of the dinoflagellate species *Apectodinium augustum* (Fig. 17) in the upper part of zone NP9 (Heilmann-Clausen and Egger, 1997; Egger et.al., 2000; Crouch et al., 2001). The onset of the CIE is characterized by the presence of the thickest hemipelagic layers of the entire Anthering Section. About 45 % of the rock is claystone, whereas the average percentage of claystone in the overlying NP10 is only 14 %, and even less in the lower part of NP9. The CIE-interval attains a thickness of 15 m, comprising turbidites and hemipelagites. The thickness of the turbidites varies between 0.08 m and 2.25 m, although only the thickest layer exceeds 1 m thickness. The average thickness of the turbidite beds is 0.39 m and sand-grade material, which makes up 2 % of this facies, occurs only in the thickest layers. Excluding the turbidites the remaining thickness of hemipelagic claystone is 8.4m. Using Fe– and Ca–intensity curves which probably represent precessional cycles, Röhl et al. (2000) calculated that the CIE interval lasted for 170 ky. From this, a hemipelagic sedimentation rate of 49 $mmky^{-1}$ has been calculated for the compacted sediment across the CIE.

This value is ca. six times higher than the hemipelagic sedimentation rate in the Paleocene (Egger et al., 2009). The increased rate of hemipelagic sedimentation at the CIE suggests a high input of siliciclastic suspension into the basin. At the level of the CIE clay mineral assemblages of hemipelagic claystone display a distinct increase of smectite and kaolinite at the expense of illite and chlorite (Egger et al., 2002). This indicates a decrease of bedrock erosion in the adjoining land areas. Well-developed smectitic soils with a mixture of kaolinite are mostly restricted to subtropical climates with a well-marked dry season (see Thiry, 2000 for a review). During the rainy season continental erosion of such areas is very pronounced (see van der Zwan, 2002, for a review) and will result in a strong increase in hemipelagic sedimentation rates (Schmitz et al., 2001).

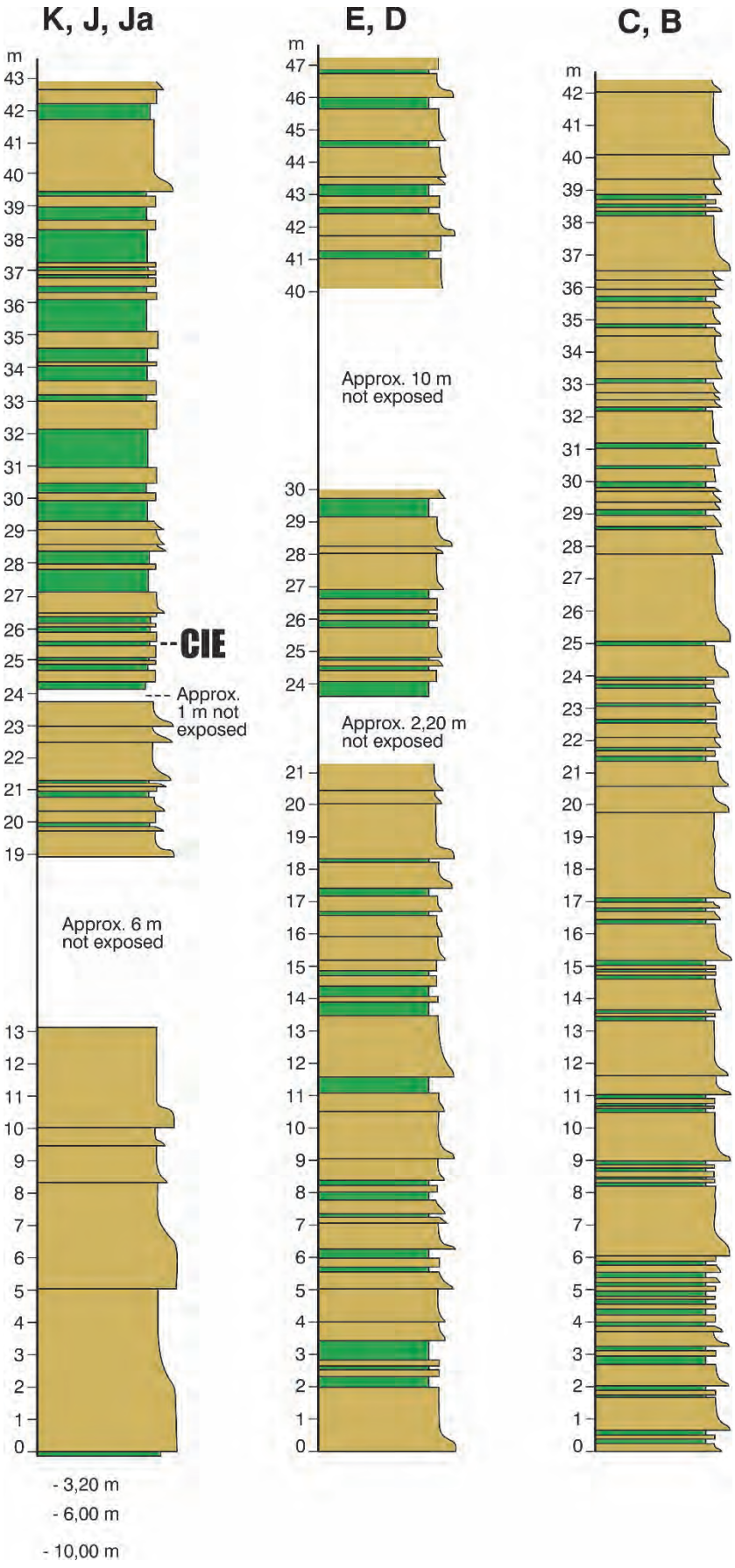

Fig. 14: Lithologic logs of outcrops at Anthering.

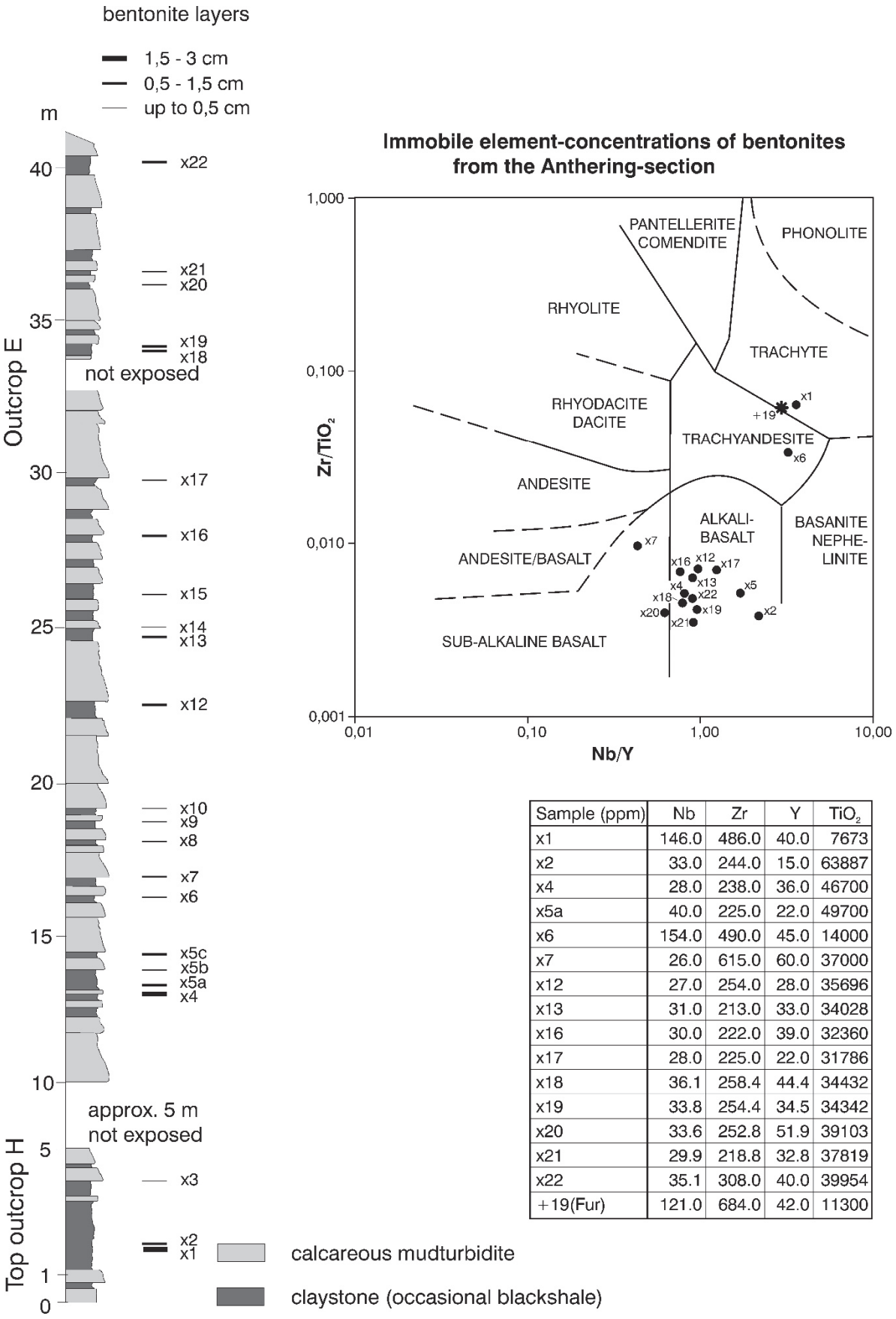

Sample (ppm)	Nb	Zr	Y	TiO_2
x1	146.0	486.0	40.0	7673
x2	33.0	244.0	15.0	63887
x4	28.0	238.0	36.0	46700
x5a	40.0	225.0	22.0	49700
x6	154.0	490.0	45.0	14000
x7	26.0	615.0	60.0	37000
x12	27.0	254.0	28.0	35696
x13	31.0	213.0	33.0	34028
x16	30.0	222.0	39.0	32360
x17	28.0	225.0	22.0	31786
x18	36.1	258.4	44.4	34432
x19	33.8	254.4	34.5	34342
x20	33.6	252.8	51.9	39103
x21	29.9	218.8	32.8	37819
x22	35.1	308.0	40.0	39954
+19(Fur)	121.0	684.0	42.0	11300

Fig. 15: Log of outcrop E showing positions of bentonites and immobile element concentrations of bentonites.

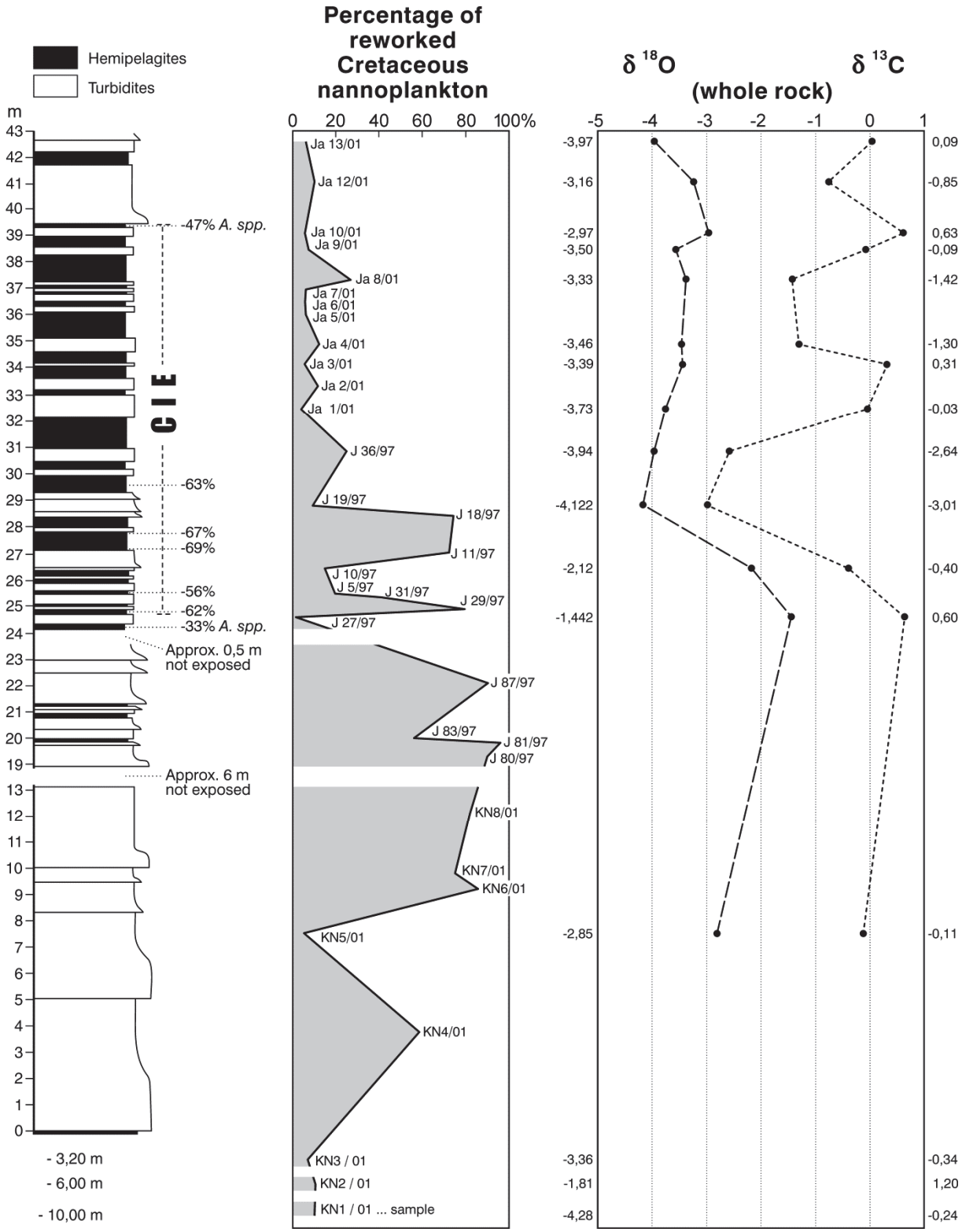

Fig. 16: Lithostratigraphy, percentages of redeposited Cretaceous nannoplankton, and stable isotope record of oxygen and carbon across the CIE-interval at Anthering. A. spp. percentages of the genus Apectodinium in the dinoflagellate assemblage (Egger et al., 2009).

Enhanced erosion of land areas around the CIE-interval can also be inferred from the composition of calcareous nannoplankton assemblages. Whereas, in general, reworked Cretaceous species form only 2-3 % of the calcareous nannoplankton assemblages of the Anthering section, substantial Cretaceous admixtures are present in many samples from across the CIE. The oldest nannoplankton assemblage showing a high percentage (>50 %) of reworked specimens originates from a turbidite bed 22 m below the onset of the CIE. Three metres above the onset of this geochemical marker, the youngest assemblage with a similar percentage of reworked Cretaceous specimens has been found (Fig. 16).

Most of the reworked specimens consist of species with a long stratigraphic ranges (*Watznaueria barnesae, Micula staurophora, Retecapsa crenulata, Cribrosphaerella ehrenbergii, Eiffellithus turriseiffelii*). Biostratigraphically important species that were found in all of the counted samples include *Broinsonia parca, Arkhangelskiella cymbiformis* (small specimens), Calculites obscurus, Lucianorhabdus cayeuxii and Eiffellithus eximius whilst *Marthasterites furcatus, Eprolithus floralis* and *Lithastrinus grillii* were found only occasionally. This assemblage suggests that predominantly lower to middle Campanian deposits were reworked at the end of the Paleocene. Probably, the erosional area was the North-Helvetic shelf at the southern European Plate where the Middle Eocene is resting with an erosional unconformity on the Upper Cretaceous.

Substantial reworking of the Cretaceous started already in the latest Paleocene. At Anthering, the uppermost 20 m of the Paleocene succession are formed by the thickest turbidites (up to 5 m) of the entire section. The siliciclastic sand-fraction in the turbidites forms around 30 % of the rocks in this part of the section (Altlengbach Formation). This suggests that a sea-level drop took place shortly before the onset of the CIE. This is consistent with data from the Atlantic region (Heilmann-Clausen, 1995; Knox, 1998; Steurbaut et al., 2003; Pujalte and Schmitz, 2006; Schmitz and Pujalte, 2007). The synchroneity of this sea-level drop in the Atlantic and Tethys regions indicates a eustatic fluctuation. Starting with the onset of the CIE, mainly fine-grained suspended material came into the basin and caused an increase in hemipelagic sedimentation rates by a factor of 5 or 6. Such an increase associated with decreasing grain-sizes has already been reported from P/E-boundary sections elsewhere and interpreted as an effect of a climate change at the level of the CIE, affecting the hydrological cycle and erosion (Schmitz et al., 2001).

Dinoflagellates

Information on the distribution of organic-walled dinoflagellate cysts in the Anthering section has previously been briefly published by Egger et al. (1997 and 2000), Heilmann-Clausen and Egger (2000) and Crouch et al. (2001). With results obtained during the present study the data can be summarized as follows. Common genera ans species occurring throughout the section are *Apectodinium* spp., *Areoligera* spp., *Glaphyrocysta* spp., *Spiniferites* spp., *Polyspaeridium zoharyi*, *Homotryblium tenuispinosum, Operculodinium centrocarpum*, and *Phthanoperidinium crenulatum*. *Lingulodinium machaeorophorum* occurs sporadically and is usually rare.

The overall composition of the dinoflagellate assemblages allows a simple subdivision of the section into three parts: The lower and upper intervals are characterized by generally low dominance and relatively high species richness. These two intervals are separated by a middle interval coinciding with the CIE (outcrops J and JA). There the genus *Apectodinium* which usually accounts for 5 % - 20 % of the dinoflagellate assemblages is dominant and reaches abundances up to 69 % in hemipelagic samples. The genus *Apectodinium* includes several intergrading species, which form a closely related group

(Harland, 1979). In spite of the strong dominance, the species richness remains relatively high within the CIE interval.

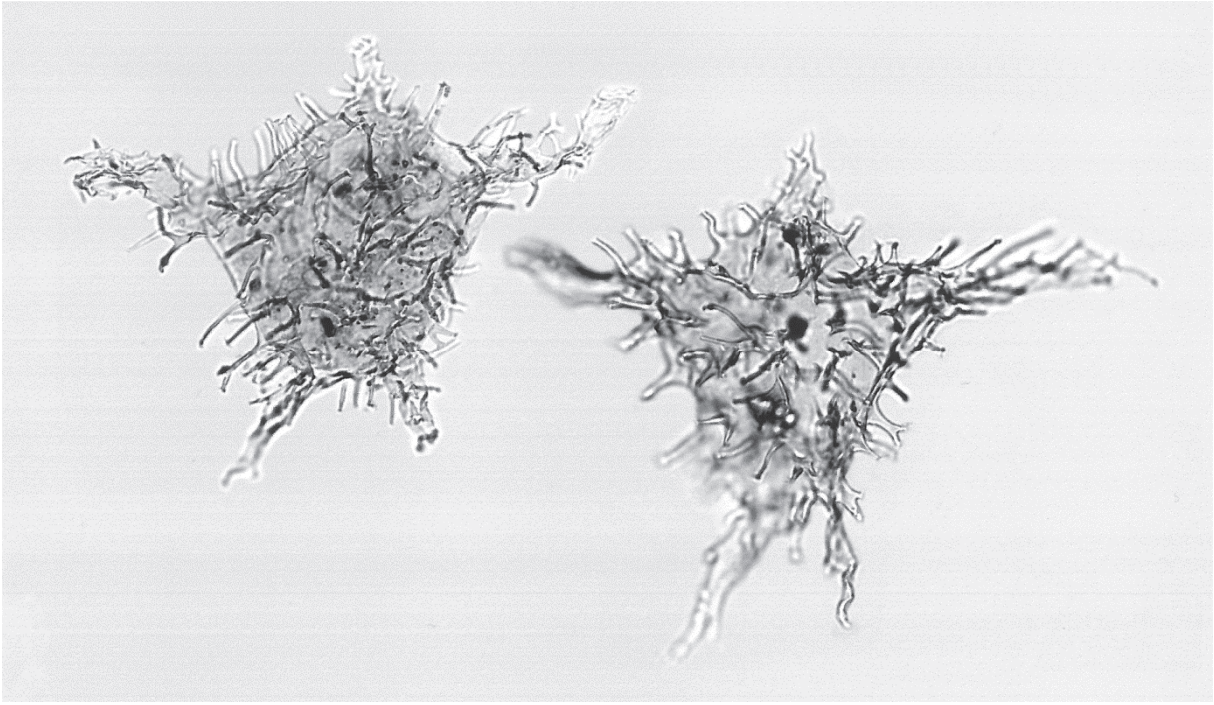

Fig. 17: Apectodinium augustum. Left specimen from Anthering, outcrop j. Right specimen from the CIE-interval in Denmark (Viborg Borehole).

Quantitative dinoflagellate cyst data from hemipelagic layers at outcrop J reveal there is a ten-fold to forty-fold increase in the total number of cysts within the CIE interval (where *Apectodinium* dominates). Above the CIE, counts reveal fluctuations in cyst numbers with a general trend towards reduction, which parallel the declining percentages of *Apectodinium*. The total number of cysts is low in sample J4 from the CIE-interval, with dominant *Apectodinium*, but this sample is from a layer with a minimum in the TOC which suggests increased oxygenation at this level. The *Apectodinium* percentages are increased in sample J26 (33 %) and J28 (62 %), but no data of absolute dinoflagellate abundances are available for these two samples.

Relying on information from modern cyst production (e.g. Dale, 1996), the Anthering Section must have been deposited below neritic waters, or waters which originated in the neritic zone. The genus *Impagidinium*, which is today purely oceanic, is present in several samples (especially in outcrop N), but usually rarer than 1-2 %. Such low occurrences indicate the neritic/oceanic boundary interval (Dale 1996). It should be noted that the boundary between neritic and oceanic waters today does not strictly follow bathymetry and presence of neritic waters need not conflict with the interpretation of the depositional environment at Anthering being an abyssal basin floor (Egger et al., 2000). It is also well known that neritic cysts are today transported over long distances with currents, and are deposited in various basinal parts of the Atlantic Ocean (e.g. Dale, 1996).

The continuous presence of *Polysphaeridium zoharyi* and *Homotryblium tenuispinosum* is evidence of a rather constant, and significant, mixing of the water masses at Anthering. *Polysphaeridium zoharyi* today mainly characterizes equatorial lagoons (Dale, 1996), and the extinct *Homotryblium* is a dominant form in several well-documented inner neritic, probably lagoonal settings of various ages

(e.g. Köthe, 1990; Brinkhuis, 1994; Dybkjær and Rasmussen, 2000; and personal observation of Heilmann-Clausen in the basal Oligocene Heide Sand, Belgium).

Siliceous plankton

Throughout the Anthering section the fossil remains of siliceous plankton (radiolaria, diatoms as well as rare ebridians and silicoflagellates) have been replaced by pyrite. Silica dissolution prior to this replacement, and damage caused by the pressure of pyrite crystals growing inside the shells, can make identification difficult. In particular, radiolarians are very poorly preserved and are all taxonomically indeterminate spheroidal or lenticular spumellarians (Christopher Hollis, oral communication). If pyrite fillings only are preserved, the outline and shape of diatom frustules can be recognized, but a specific and often generic determination is impossible. However, in the more robust frustules, even relatively fine pores and cribra covering the areolae are preserved, and thus allow species determination.

Most samples have diatom floras dominated by the taxa *Paralia sulcata* var. *biseriata*, *Paralia sulcata* var. *crenulata*, *Coscinodiscus antiquus*, and by species of the genera *Auloplicata* and *Stephanopyxis*. The recent relatives of the latter two genera occur in coastal-neritic as well as in oceanic environments. This may also be the case for the less common species of the genera *Hemiaulus* (e.g. H. *peripterus*), *Actinoptychus* and *Sceptroneis*. Species of the genus *Trochosira*, which are also rather rare, are considered to have been fully planktonic, whereas specimens of *Craspedodiscus*, *Trinacria*, *Sheshukovia* and *Aulacodiscus* probably indicate a coastal-neritic environment. Other genera can be considered to have been fully benthic, e.g. species of the genera *Auliscus* and *Arachnodiscus*. In neritic assemblages, resting spores should be abundant, but in the studied samples only single specimens of resting spores were found. These belong to the form groups *Xanthiopyxis*, *Pterotheca* and *Bicornis*. As resting spores are most resistant to dissolution, their scarcity indicates that the encountered diatoms represent an oceanic assemblage (Fenner, 1994). The minor admixture of coastal and neritic specimens may have been caused by storm events that whirled up freshly deposited sediment in shallow regions which thereafter settled out from suspension beyond the shelf edge.

The occurrence of *Craspedodiscus* spp. and *Trinacria* spp. in deep-water deposits at Anthering is highly remarkably as these genera are usually restricted to neritic environments. We can rule out redeposition of these specimens because in that case, resting spores and benthic species would have been redeposited in considerable amounts. This suggests that water-depth was not the limiting factor for the occurrence of *Craspedodiscus* spp. and *Trinacria* spp.. Probably, the preference of these genera for neritic settings was due to the higher level of dissolved nutrients in these areas.

Agglutinating foraminifera

Individual samples contain up to 65 species and more than 700 specimens agglutinated foraminifera. More than 90 species were identified and grouped into four morphogroup assemblages (tubular genera, infaunal passive deposit feeders, active deposit feeders, epifaunal active herbivores and omnivores). Distributional patterns of morphogroups of agglutinating foraminifera are related, more or less directly, to food supply and food utilisation processes (Jones and Charnock, 1985).

At Anthering, tubular forms comprise the genera *Nothia*, *Rhabdammina*, *Rhizammina*, *Psammosiphonella* and *Bathysiphon*. These typical „flysch-type“ elements have been interpreted as sessile suspension feeders (morphogroup A of Jones and Charnock). However, the ecological interpretation of some of these deep-sea genera is still under discussion (Gooday et al., 1997), e.g. the life habitat of *Nothia* has been re-interpreted as epibenthic detrivore (Geroch and Kaminski, 1992).

Epi- and infaunal passive deposit feeders (morphogroup B1) comprise *Saccammina*, *Psammosphaera*, *Hormosina*, *Hormosinella*, *Trochamminoides*, *Paratrochamminoides*, *Lituotuba*, *Hyperammina* and *Kalamopsis*. Another epifaunal and shallow infaunal group of active deposit feeders (morphogroup B2) corresponds to the *Ammodiscus* - *Glomospira* assemblage of „Biofacies B" (Kuhnt et al., 1989). It consists of the genera *Ammodiscus*, *Glomospira* and *Rzehakina*. The B3 assemblage of epifaunal active herbivores and omnivores (*Haplophragmoides*, *Trochammina* s.l.) may be restricted to omnivores in this deep-sea environment. The C-morphogroup of infaunal forms (*Gerochammina*, *Karrerulina*, *Reophax*, *Subreophax*, *Spiroplectammina*) are negligible in the abyssal setting of the Anthering section. The genera *Recurvoides* and *Thalmannammina* were summarized as *Recurvoides*-assemblage. The microhabitat preferences of this assemblage are questionable. In the Cretaceous „Hatteras Fauna" of the Fardes Formation in southern Spain it co-occurs with *Glomospira* and *Ammodiscus*, and might, therefore, be indicative of oxygen deficient conditions (Kaminski et al., 1999). In our samples we did not find this correlation because the highest percentages of the *Recurvoides*-assemblage occur in high diversity faunas without any indication of oxygen depletion. It is noteworthy, that the *Recurvoides*-assemblage usually forms more than 10% of the agglutinated faunas within nannoplankton zone NP9 whereas in zone NP10 this percentage is much lower.

The highest diversity and the highest abundance of agglutinated specimens occur in the lower part of the section (samples NF2 to LF1). These assemblages display balanced proportions of infaunal, epifaunal and suspension feeding species. The high diversity of these agglutinated faunas is seen as typical for oligotrophic, food-limited environments where the various microhabitats are fully occupied. Several taxa have their last occurrences in this part of the section: *Ammodiscus cretaceus, Aschemocella* cf. *carpathica, A. grandis, Haplophragmoides horridus, H. suborbicularis, Hormosina trinitatensis, Karrerulina* cf. *coniformis, Paratrochamminoides heteromorphus, P. multilobus, Recurvoides walteri, Remesella varians, Rzehakina complanata, R. epigona, R. fissistomata, Spiroplectammina* cf. *dentata, Spiroplectammina spectabilis, Thalmannammina n. sp., Thurammina papillata.*

Further up-section (samples J85 to JaF1) impoverished faunas with a predominance of the genus *Glomospira* appear. This "*Glomospira* event" has been observed at numerous localities in the Tethys and northern North Atlantic (see Kaminski et al., 1996 for a review). Kaminski et al. (1989) speculated that the predominance of *Glomospira* indicates areas of high surface productivity that caused low-oxygen levels at the sea-floor. However, this assemblage occurs also in well oxidized sediments and, therefore, it may be opportunistic rather than a reliable indicator for high productivity (Galeotti et al., 2000; Kaminski et al., 1996). With the onset of the CIE, even this opportunistic assemblage disappeared and over a period of at least 180 000 years the benthic communities suffered severely from unfavorable habitat conditions.

Between samples HF2 to EF1 the majority of the hemipelagic layers have an organic carbon content between 0.14% and 0.17% (0.15% on average), but several black shale layers (up to 1.22% TOC) occur. This suggests periodic eutrophication of the sea water probably by volcanic ashfall as closely spaced bentonites were found in that part of the section (Egger et al., 2000). The black shales are usually devoid of benthic foraminifera and contain common framboidal pyrite indicating anoxic conditions (Egger et al., 1997). The agglutinating faunas of these layers are not as rich and diverse as those from further down the section. *Glomospira glomerata* has its first appearance in this part of the section. The faunal assemblage changed to a predominance of passive deposit feeders (B1-assemblage) and tubular

genera (A-assemblage). These assemblages are dominant along the continental rises where bottom currents or distal turbidity currents occur (Kaminski et al., 1996).

In the uppermost part of the Anthering section (samples DA64a to BF1) a strong increase in the number of species and specimens of the DWAF, with relatively balanced assemblages, occurs indicating the return of ecological conditions similar as those at the base of the section.

Stop 3 Frauengrube Section near St. Pankraz

Hans Egger

Topic: Erosional unconformity between the Thanetian and Ypresian
Tectonic unit: South Helvetic nappe complex (European Plate)
Lithostratigraphic unit: Kressenberg Formation, Fackelgraben Member, Frauengrube Member
Chronostratigraphic units: Thanetian, Ypresian
Biostratigraphy: Calcareous Nannoplankton Zones NP9 and NP12
Location: Frauengrube Quarry (Fig. 6C)
Coordinates: 47° 56´ 11“ N, 013° 00´ 06“ E
References: Egger et al., 2009, Rasser & Piller, 1999 and 2001

In the Haunsberg area, the Frauengrube section and the immediately adjoining Kroisbach section are both part of the South-Helvetic nappe complex. The base of the succession is a grey mica-bearing marlstone of the Maastrichtian Gerhartsreit Formation, which is overlain by silty claystones and clayey siltstones of the Paleocene Olching Formation. Detailed nannoplankton studies at the Cretaceous/Paleogene-boundary indicate continuous sedimentation across the boundary, since the uppermost Maastrichtian (*Micula prinsii* Zone) and the lowermost Paleocene (*Markalius inversus* Zone) have been discovered (Stradner, pers. comm. 2005). Around the boundary, the amount of terrestrially-derived sediment input strongly increases at the expense of carbonate. This shift in the lithological composition defines the lithostratigraphic boundary between the Gerhartsreit and Olching formations.

The Olching Formation is overlain by the Kroisbach Member of the Kressenberg Formation. This member is characterized by glauconite-bearing quartz-sandstones with abundant brachiopods (*Crania austriaca* Traub) in the lower part and oysters (*Pycnodonte* spp.) in the upper part. The glauconitic matrix of the oyster-beds contains calcareous nannoplankton of the Upper Thanetian *Heliolithus riedelii* Zone (NP8) and very well preserved pollen and spores (Stradner, in Gohrbandt, 1963; Kedves, 1980; Draxler, 2007).

The Kroisbach Member is overlain by the rhodolithic limestone of the Fackelgraben Member (Figs. 18 and 19). Samples from thin intervening marlstone layers in the upper part of this member contained poorly preserved calcareous nannoplankton of the *Discoaster multiradiatus* Zone (NP9), of latest Paleocene age: *Chiasmolithus* sp., *Coccolithus pelagicus*, *Discoaster falcatus*, *Discoaster multiradiatus*, *Discoaster mohleri*, *Fasciculithus tympaniformis*, *Neochiastozygus perfectus*, *Thoracosphaera* sp., *Toweius callosus*, *Toweius pertusus*. Reworking of Cretaceous species has not been observed.

The Fackelgraben Member and the overlying Frauengrube Member are separated by an irregular erosional surface (Fig. 20), that has been described previously from other outcrops in the Salzburg area (Vogeltanz, 1977). Clasts of the Fackelgraben Member are reworked in the basal part of the Frauengrube Member (Rasser and Piller, 2001), which comprises 0.5 m of brownish sandstone with a

marly matrix, that contains poorly preserved calcareous nannoplankton. Reworked species from the Campanian and Maastrichtian make up about 5% of the nannoplankton assemblage (*Arkhangelskiella cymbiformis, Broinsonia parca, Cribrosphaerella ehrenbergii, Cyclagelosphaera reinhardtii, Eiffellithus eximius, Markalius inversus, Micula staurophora, Prediscosphaera cretacea, Watznaueria barnesae*). The rest of the species observed have their first occurrence during the Paleocene (*Campylosphaera eodela, Chiasmolithus bidens, Chiasmolithus consuetus, Chiasmolithus danicus, Coccolithus pelagicus, Discoaster barbadiensis, Discoaster multiradiatus, Thoracosphaera* sp., *Toweius spp*.) or in the lower Eocene (*Neochiastozygus junctus, Pontosphaera versa, Pontosphaera duocava, Rhabdosphaera solus, Transversopontis pulcher, Zygrhablithus bijugatus*). Unfortunately, no marker species of the lowermost Eocene, in particular of the *Rhomboaster-Tribrachiatus* lineage, have been encountered in our samples. However, *Tribrachiatus orthostylus* (Type B = without bifurcated rays) has been described from the base of the Frauengrube Member from another outcrop in the Haunsberg area (Stradner in Gohrbandt, 1963). This finding indicates that the onset of the transgression did not take place before the *Discoaster binodosus* Zone (NP11).

Beside calcareous nannoplankton, the samples from the base of the Frauengrube Member contain marine and terrestrial palynomorphs. The terrestrial flora indicates a subtropical to tropical climate containing Sapotaceae and Matixiaceae pollen among other floral elements (*Dictyophyllidites* sp., *Pityosporites* sp., *Nudopollis* sp., *Subtriporopollenites* sp., *Cupuliferoidaepollenites liblarensis*). Palmpollen have not been found (Draxler, pers. comm. 2006).

The marine flora contains very similar, relatively well preserved dinoflagellate assemblages dominated by *Homotryblium tenuispinosum ("tasmaniense*-type"), *Polysphaeridium zoharyi* and *Apectodinium* spp. (excluding *A. augustum*). The three taxa are equally common, and together are estimated to constitute 60-90% of the dinoflagellate assemblages. Of relevance for age-determination is the occurrence of the *Areoligera undulata – A. sentosa* group (present in each sample), *Glaphyrocysta* cf. *semitecta* (samples 1 and 3), *Deflandrea oebisfeldensis* (2 specimens in sample 1) and *Phthanoperidinium* cf. *echinatum* (1 or 2 specimens in sample 1). In addition to these taxa, the samples also include low abundances of several long ranging taxa without stratigraphic value. *Spiniferites* spp. and *peridinioids*, apart from *Apectodinium*, are rare.

The *Areoligera undulata – A. sentosa* group, *Glaphyrocysta* cf. *semitecta* and *Phthanoperidinium* cf. *echinatum* were not recorded in the Anthering Formation at Anthering, from where dinoflagellates were previously studied (Egger et al., 2000; 2003). This suggests a younger age for the Frauengrube Member. The *Areoligera undulata – A. sentosa* group is probably of inner neritic-lagoonal origin and has previously been recorded in the Lutetian in southern England (Eaton, 1976; Bujak et al., 1980). Little is known about its stratigraphical distribution elsewhere. The several specimens of *Glaphyrocysta* (cf.) *semitecta* are very close to, but perhaps not identical with *Glaphyrocysta semitecta*, a taxon previously recorded from NP15 to near the Eocene/Oligocene boundary in NW Europe (e.g. Bujak et al., 1980; Heilmann-Clausen and Van Simaeys, 2005). Nothing else in the samples suggests such a young age. The abundance of *Apectodinium* points to an age no younger than the Ypresian-Lutetian transition, most likely early Ypresian or older. The two specimens of *Deflandrea oebisfeldensis* also point to an early Ypresian or older age, as this form becomes extinct in the lower Ypresian in NW Europe (probably in or near top of NP11, e.g. Heilmann-Clausen and Costa, 1989; Luterbacher et al., 2004).

In summary, the calcareous nannoplankton and dinoflagellate assemblages of the Frauengrube section indicate an erosional gap across the P/E-boundary, spanning the upper part of zone NP9, the entire zone NP10, and at least a large part of zone NP11.

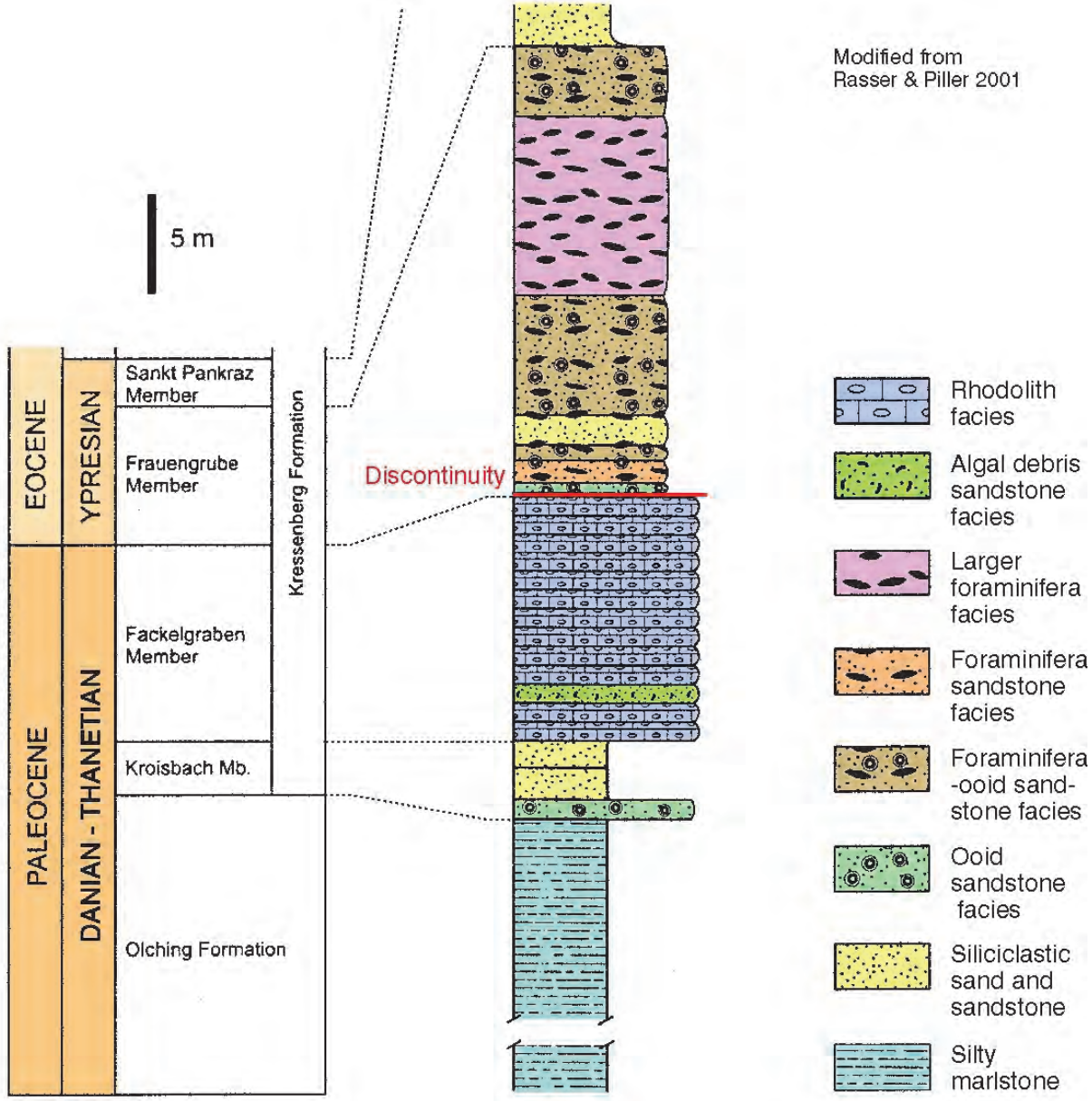

Fig. 18: Lithologic log of the Paleogene of the South Helvetic sucession in Salzburg.

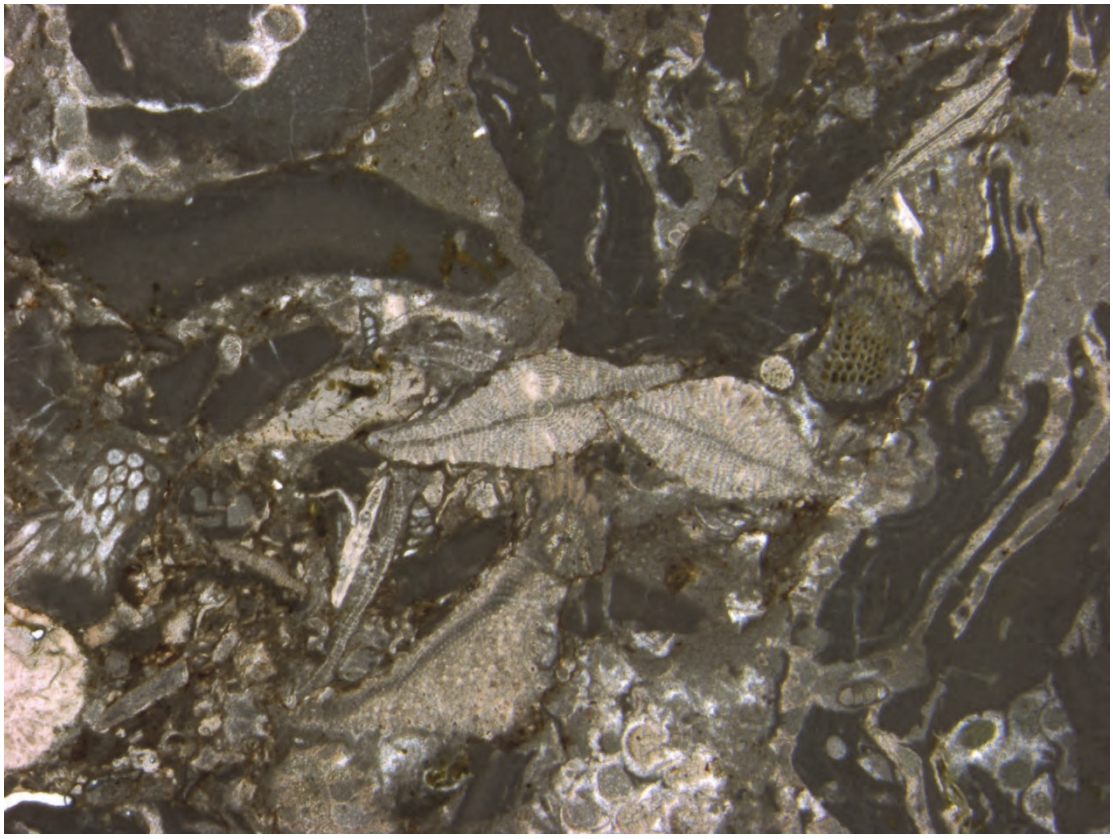

Fig. 19: Image of a thin section of rhodolithic limestone with Discocyclina sp. (Fackelgraben Member).

Fig. 20: Photograph of the type locality of the Frauengrube Member (Note the erosional unconformity between the Fackelgraben Member (left) and the Frauengrube Member (right).

Stop 4 Wimmern Section

Hans Egger

Topics: Transgression of the Adelholz Formation on the Gerhardtsreit Formation
Tectonic unit: North Helvetic Nappe Complex (European Plate)
Lithostratigraphic units: Adelholz Formation, Gerhardtsreit Formation
Chronostratigraphic units: Maastrichtian, Lutetian
Biostratigraphy: Calcareous nannoplankton Sub-Zones NP15a and NP15b
Location: Outcrops near Wimmern (Fig. 21)
Coordinates: 47° 52´ 09" N, 012° 49´ 57" E
References: Egger, H. et al. (2011)

At Wimmern (Fig. 21), the Maastrichtian is overlain by 4 m thick glauconite rich sand of the lower Adelholzen beds (Fig. 22). Poorly preserved calcareous nannoplankton assemblages from the basal 50 cm of the sand contain *Chiasmolithus grandis, Chiasmolithus solitus, Cyclicargolithus floridanus, Nannotetrina cristata*, and *Sphenolithus spiniger*, indicating calcareous nannoplankton Sub-Zone NP15a at the base of the Adelholzen beds. *Chiasmolithus gigas,* the index species for Sub-Zone NP15b has its first occurrence 4 m above the transgressional surface and is still present at the top of the section (7.5 m above the transgressional surface). Sub-Zone NP15b is presented by marlstone containing high numbers of larger foraminifera and foraminiferal limestone.

The poor preserved planktonic foraminifera assemblage from the glauconitic sand at the base of the section yields *Acarinina coalingensis*, *A. esnehensis, A. interposita, Igorina broedermanni*, and *Pseudohastigerina wilcoxensis*. Fifty centimetres above the transgression *Acarinina bullbrooki, A. cuneicamerata,* and *Pseudohastigerina micra* have their first occurrences. The assemblage suggests an assignment to planktonic foraminiferal Zone E7 in the zonation scheme of Wade et al. (2011).

The age of the transgression of the Adelholzen beds (which is called Bürgen Formation in Switzerland) is equivalent to the age of the transgression of the Lutetian at the Lutetian stratotype (St. Leu d´Esserent in the Paris Basin) where Aubry (1991) attributed the base of the type Lutetian to calcareous nannoplankton Subzone NP14b. Contrary to previous opinions (e.g. Hagn et al., 1982), this suggests that the North-Helvetic domain was affected by an eustatic sea-level rise in the Lutetian and not by tectonic subsidence.

Stop 5 Goppling section

Hans Egger

Topics: Cretaceous-Paleogene transition in an active tectonic deep-water setting. Slope basin formation on the bathyal to abyssal southern slope of the European Plate.
Tectonic unit: Ultrahelvetic Nappe Complex (European Plate)
Lithostratigraphic units: Buntmergelserie, Achthal Formation (type locality)
Chronostratigraphic units: Upper Maastrichtian to Ypresian
Biostratigraphy: Calcareous nannoplankton Zones CC26 to NP11
Location: Stecherwald southwest of Teisendorf (Fig. 23)
Coordinates: 47° 50´ 51" N, 012° 47´ 42" E (base of the section)
References: Egger, H. & Mohamed, O. (2010)

The type area of the Achthal Formation is the forest ("Stecherwald") southwest of Teisendorf. The base of the composite type section of the Achthal Formation (Goppling section) is located in creek 3 ("Gopplingbach"), ca. 15 m south of the hiking trail bridge. Further up-stream the Danian, Selandian and lower Thanetian all show excellent exposures, which end at the hamlet of Goppling. The upper Thanetian is seen only in small and poor exposures, in the two gullies east of creek 3 (Fig. 23). The Eocene part of the section is well exposed along creek 4, with the first outcrop ca. 20 m downstream from the hiking trail (coord. E 012° 48´ 02", N 47° 50´ 48").

The lithostratigraphic term "Achthaler Sandstein" dates back to Gümbel (1862, p.616). Although Schlosser (1925, p.167) mentioned a Thanetian macrofauna from this unit ("Achthaler Grünsand"), it can be assumed that these fossils originated from the tectonically neighbouring shallow-water deposits of the South-Helvetic thrust unit. Ganss and Knipscheer (1956) report on Paleocene foraminifera faunas and interpreted the outcrops as a special facies (Teisendorf facies) of the Helvetic sedimentation area. Hagn (1960 and 1967) recognized the deep-water character of the deposits and assigned them to the southern part of the Ultrahelvetic sedimentation area, which interpretation is adopted by Egger & Mohamed (2010), who introduced the term "Achthal Formation" for the deep-water turbidite succession. The base of the Achthal Formation (coord. E 012° 47´ 42", N 47° 50´ 51"), which conformably overlies the Buntmergelserie, is defined by the onset of turbiditic sedimentation in the uppermost Maastrichtian. The stratigraphic top is unknown because of the tectonic truncation of the Goppling section. However, deposition of the Achthal Formation probably ended in the Ypresian because grey calcareous marlstone of early Lutetian age occurs in the Ultrahelvetic thrust unit at Mattsee in Austria (Rögl and Egger, 2010), only ca. 25 km northeast of Teisendorf.

Fig. 21: Location of the Wimmern outcrop.

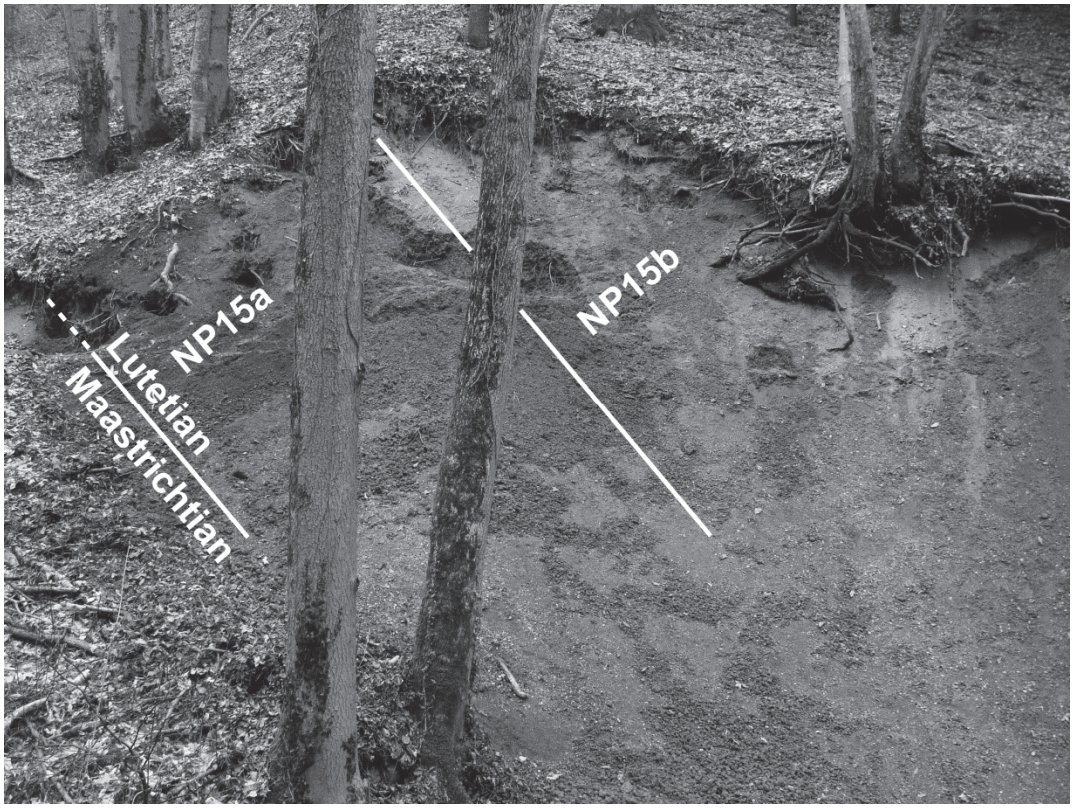

Fig. 22: Photograph of the Wimmern outcrop.

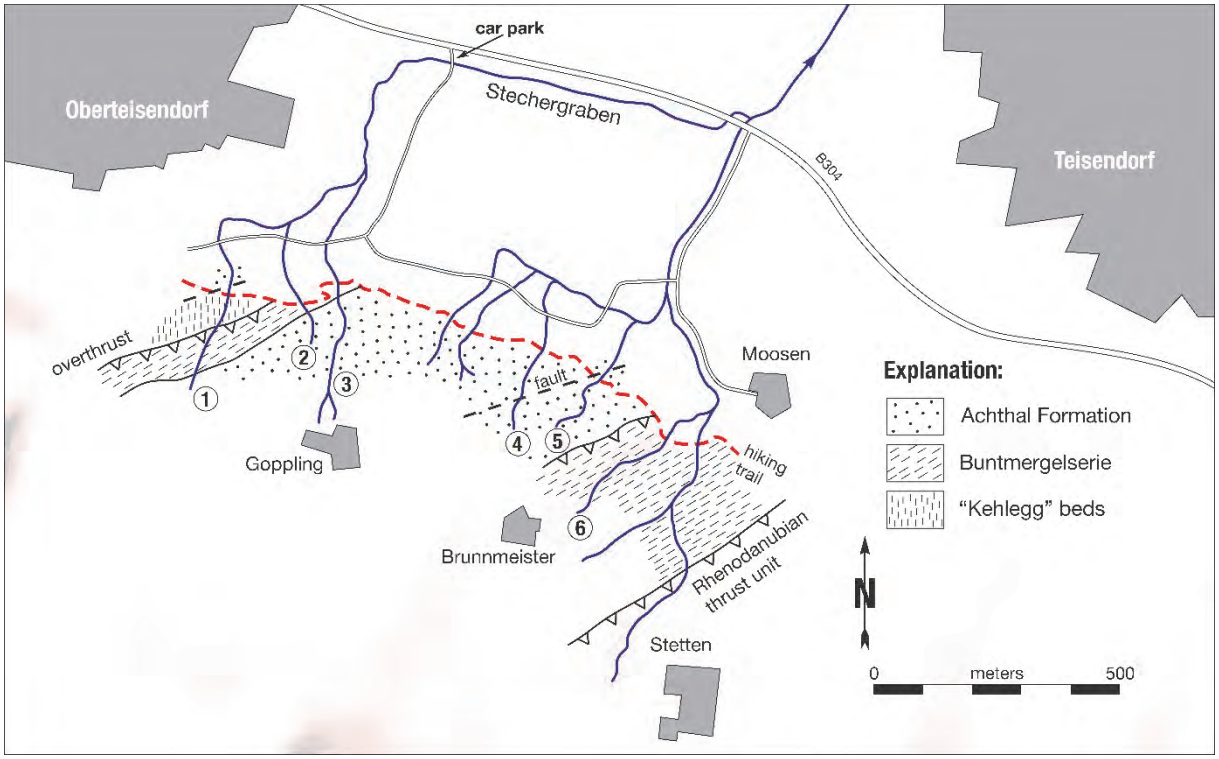

Fig. 23: Sketch map of the area investigated. Numbers indicate the most important creek sections mentioned in the text.

The deep-water system of the Achthal Formation is interpreted to have initially filled a slope depression lying above a subsiding basement fault block. Initial subsidence occurred in the latest Maastrichtian and continued into the early Paleogene. Synsedimentary tectonic activity was the primary control on the depositional evolution of the slope-basin.

In the forest south of Teisendorf and Oberteisendorf, a number of small creeks have created excellent exposures of the Achthal Formation. Almost all such outcrops lie to the south of the hiking trail running between the two villages. For better orientation, the more important creeks have been numbered (Fig. 23). The Ultrahelvetic nappe complex in the area is composed of three tectonic slices exposing beds continuously dipping to the southeast. During the field trip we will see part of the ca. 320 m thick sedimentary succession of the Goppling slice, which comprises Maastrichtian to lower Eocene deposits (Fig. 24).

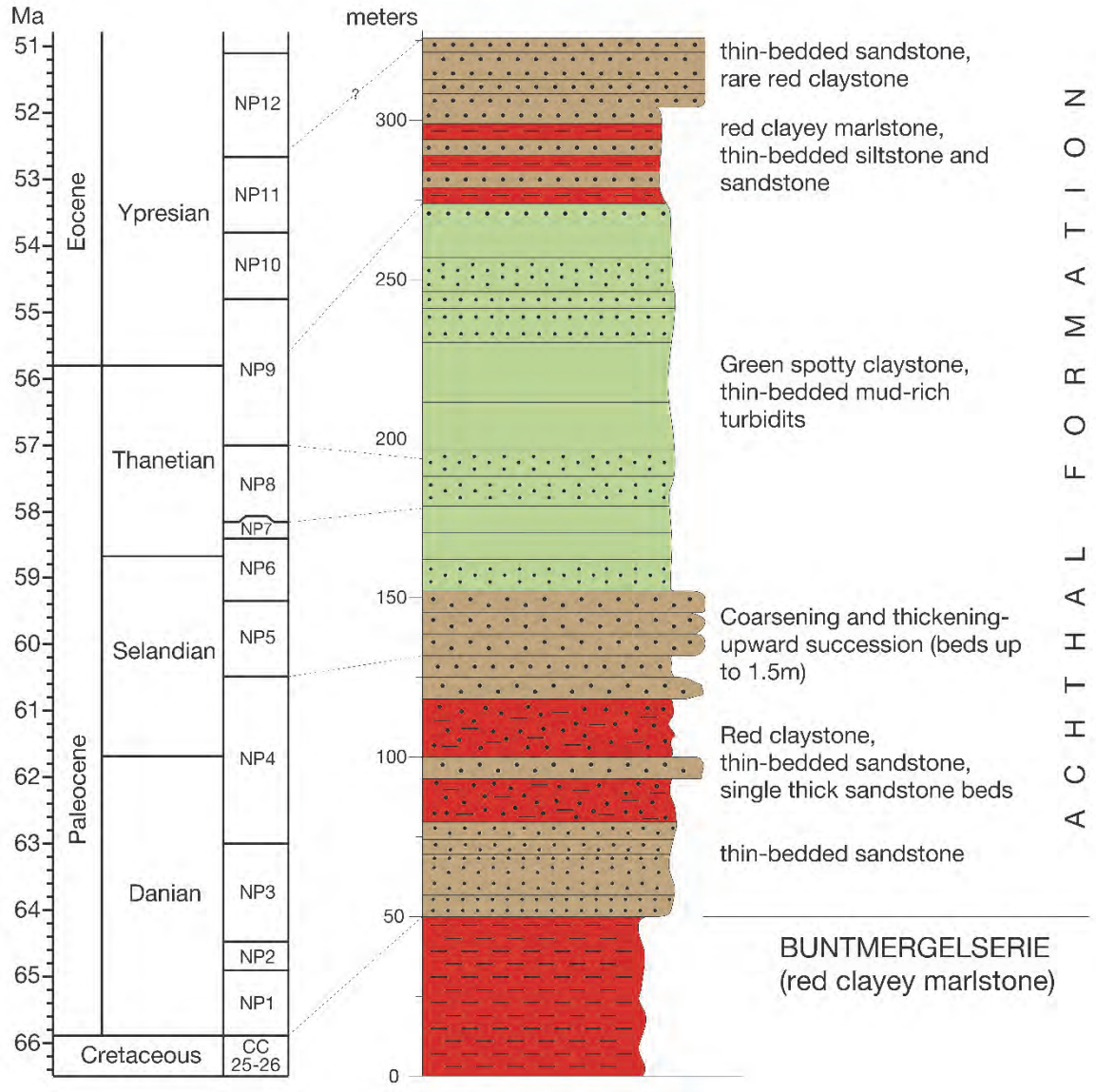

Fig. 24: Composite log of the Achthal Formation in the type area.

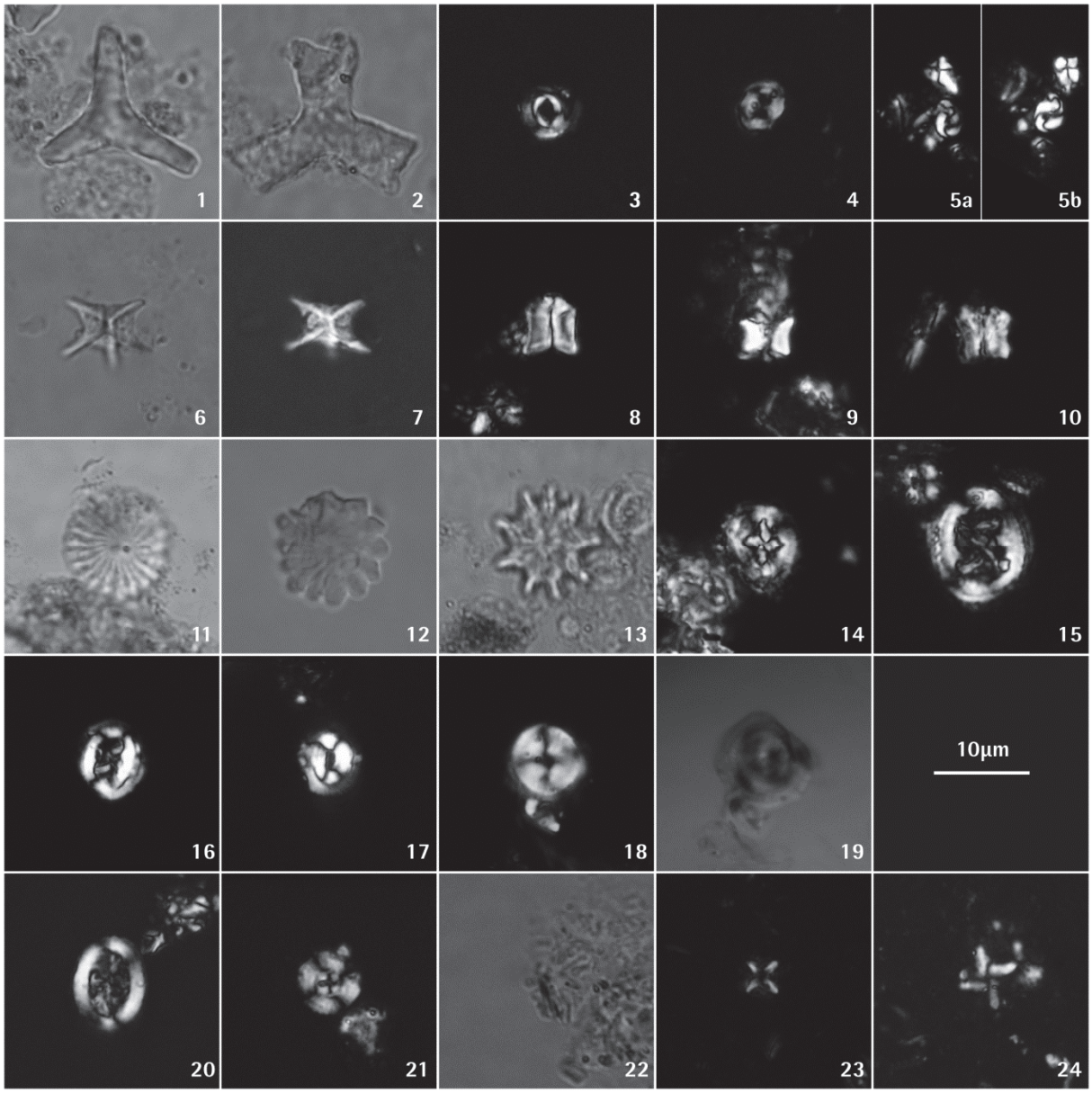

Fig. 25: Calcareous nannoplankton from the Goppling section.

Paleogene species: 1) Tribrachiatus orthostylus - Gstetten18/09; 2) Tribrachiatus digitalis – Gstetten10/09; 3) Toweius callosus – Gstetten22/09; 4) Toweius occultatus - Gstetten22/09; 5 a and b) Sphenolithus anarrhopus – Achthal 12/09; 6 and 7) Rhomboaster cuspis – Gstetten22/09; 8) Fasciculithus tympaniformis – Achthal12/09; 9) Fasciculithus billii – Achthal28/09; 10) Fasciculithus ulii – Achthal28/09; 11) Discoaster multiradiatus – Gstetten13/09; 12) Discoaster mohleri .- Achthal12/09; 13) Discoaster falcatus - Gstetten13/09; 14) Cruciplacolithus tenuis – Achthal12/09; 15) Chiasmolithus bidens – Achthal12/09; 16) Chiasmolithus danicus - Achthal12/09; 17) Coccolithus pelagicus - Achthal12/09; 18 and 19) Bomolithus elegans - Achthal28/09.

Maastrichtian: 20) Arkhangelskiella cymbiformis - Achthal18/09; 21) Ceratolithoides cf kamptneri - Achthal18/09; 22) Cyclagelosphaera reinhardtii - Achthal18/09; 23) Micula staurophora - TS10/09; 24) Micula prinsii - TS10/09.

Stratigraphic Framework of the Goppling Section

Maastrichtian

The basal part of the Goppling section is formed by ca. 50 m of bioturbated red clayey marlstone, which is assigned to the Buntmergelserie. The top of this red-bed succession is exposed in creek 3 ("Goppling creek"), immediately south of the hiking trail bridge. There, the marlstone contains 19 wt% carbonate. The nannoplankton assemblages are dominated by *Micula staurophora*, whereas all other species are rare and most specimens are preserved only as fragments. Apart from *Lithraphidites quadratus*, the zonal marker for the upper Maastrichtian Zone CC25, *Arkhangelskiella cymbiformis* (Fig. 25/20), *Cyclagelosphaera reinhardtii* (Fig. 25/22), *Eiffellithus turriseiffeli*, *Micula staurophora*, *Prediscosphaera cretacea, Retecapsa crenulata*, and *Watznaueria barnesae* occur. At the top of the red marlstone outcrop, small specimens of *Ceratolithoides* cf *kamptneri* were observed (Fig. 25/21), indicating already Zone CC26.

Two samples for foraminifera studies were taken from the red marlstone at the outcrop in creek 3 outcrop. The assemblages consist essentially of a rich agglutinated fauna and a small number of calcareous benthic species. Very small planktic species were found only in one sample and display excellent grain-size sorting suggesting reworking by current activity.

Predominant dissolution-resistant species in the calcareous nannoplankton assemblages and the composition of foraminifera assemblages indicate sedimentation of the Maastrichtian red clayey marlstone in a deep-water environment. The absence of an authochthonous planktic fauna indicates deposition below the foraminiferal lysocline, where all planktic foraminifera are dissolved (Berger, 1970). Below the lysocline and above the calcite compensation depth (CCD) calcareous nannoplankton form coccolith ooze, because in spite of their small size, some coccoliths are more dissolution-resistant than foraminifera (see Hay, 2004, for a review).

In the latest Maastrichtian (*Micula prinsii*-Zone), rapid subsidence brought the Ultrahelvetic sea-floor to below the CCD. The red marlstone transitionally passes into ca. 5 m of grey marlstone with intercalated thin carbonate-cemented parallel-laminated turbiditic siltstone and sandstone beds. The best outcrop of these rocks was found in creek 2 about 10 m south of the hiking trail. In the lower part of this outcrop, carbonate values of three samples (TS2/09, TS7/09 and TS9/09) range between 20.8 wt% and 21.5 wt%. In the upper part carbonate values decrease to 9.4 wt% (TS10/09) and finally to less than 2 wt% (TS12/09, TS13/09 and TS14/09). Dinoflagellate cyst assemblages indicate a Maastrichtian age of the claystone as in the uppermost sample *Dinogymnium acuminatum* occurs (Fig. 26/1), which does not cross the K/Pg-boundary (e.g. Stover et al. 1996).

Associated with this regional subsidence along the southern continental margin of the European Plate, was the onset of turbidite sedimentation. Turbidity currents running parallel with the strike of the slope indicate an opposing topographic high, which caused deflection of the down slope sediment transport (Kneller and McCaffrey, 1999). Subsidence of the sea-floor associated with the deposition of sediment-gravity flows and the coeval generation of a sea-ward bounding topographic high suggest the formation of an intra-slope basin on subsiding crustal fault blocks.

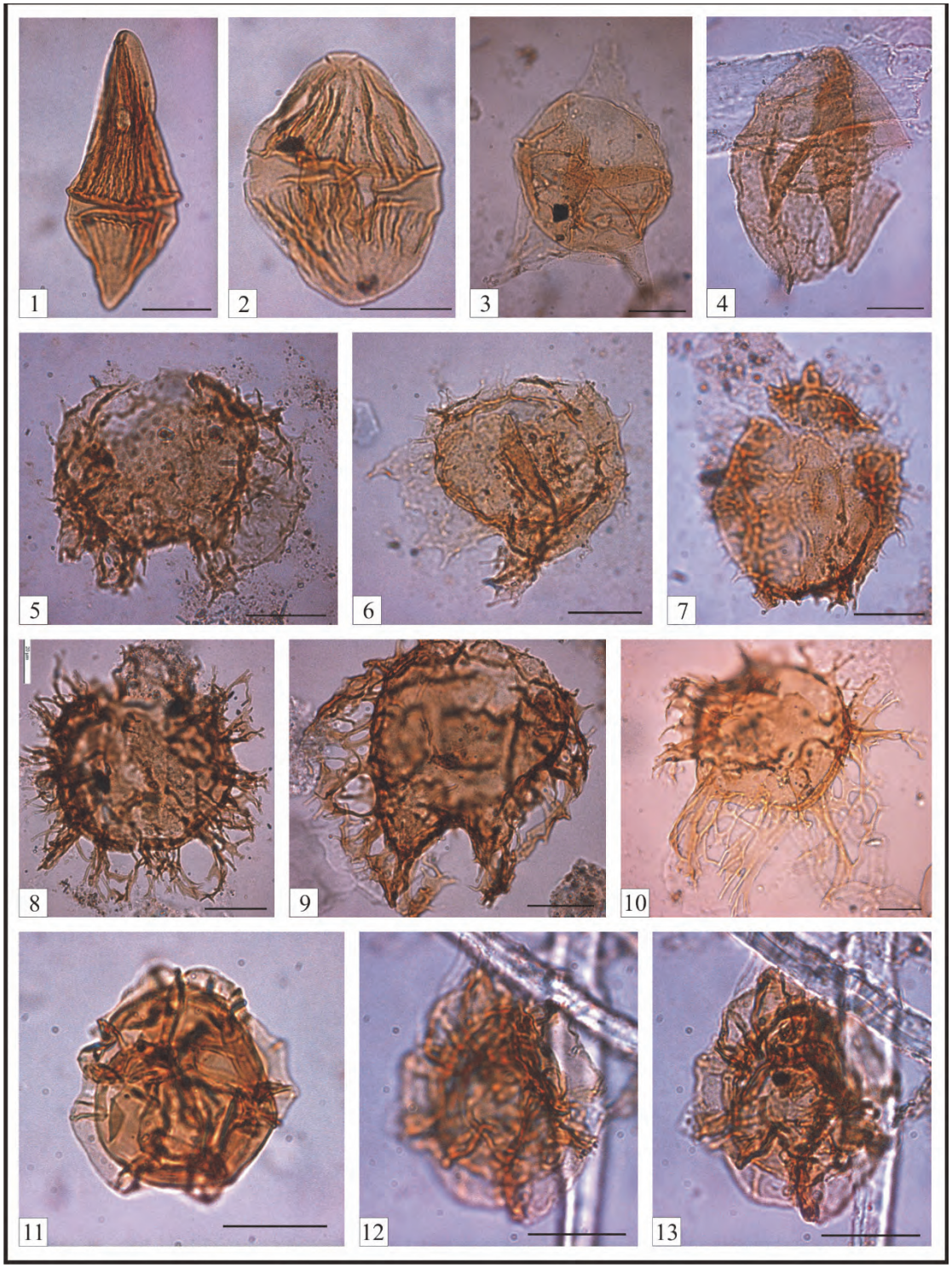

Fig. 26: Dinoflagellate taxa from the Goppling section. The species name is followed by sample location and England Finder coordinates (for localization of the specimen on the slide). Scale is 20 µm. 1) Dinogymnium acuminatum - TS11/09/a, O24; 2) Dinogymnium sp., TS11/09/a, F7/3; 3) Cerodinium sp, TS11/09/a, X16/3; 4) Trithyrodinium suspectum - TS8/09/a, B24/2; 5) Palynodinium grallator - TS13/09/a, C40; 6) Palynodinium grallator - TS11/09/a, W36; 7) Palynodinium minus - TS13/09/b, Y27; 8) Areoligera volata - Ach.2/09/a, G12; 9) Areoligera coronata - Ach.1/09/a, A3; 10) Areoligera gippingensis - TS11/09/a, X34; 11) Pterodinium cingulatum subsp. cingulatum - TS12/09/a, W33/4; 12 and 13) Pterodinium aliferum - TS8/09/a, D6/1.

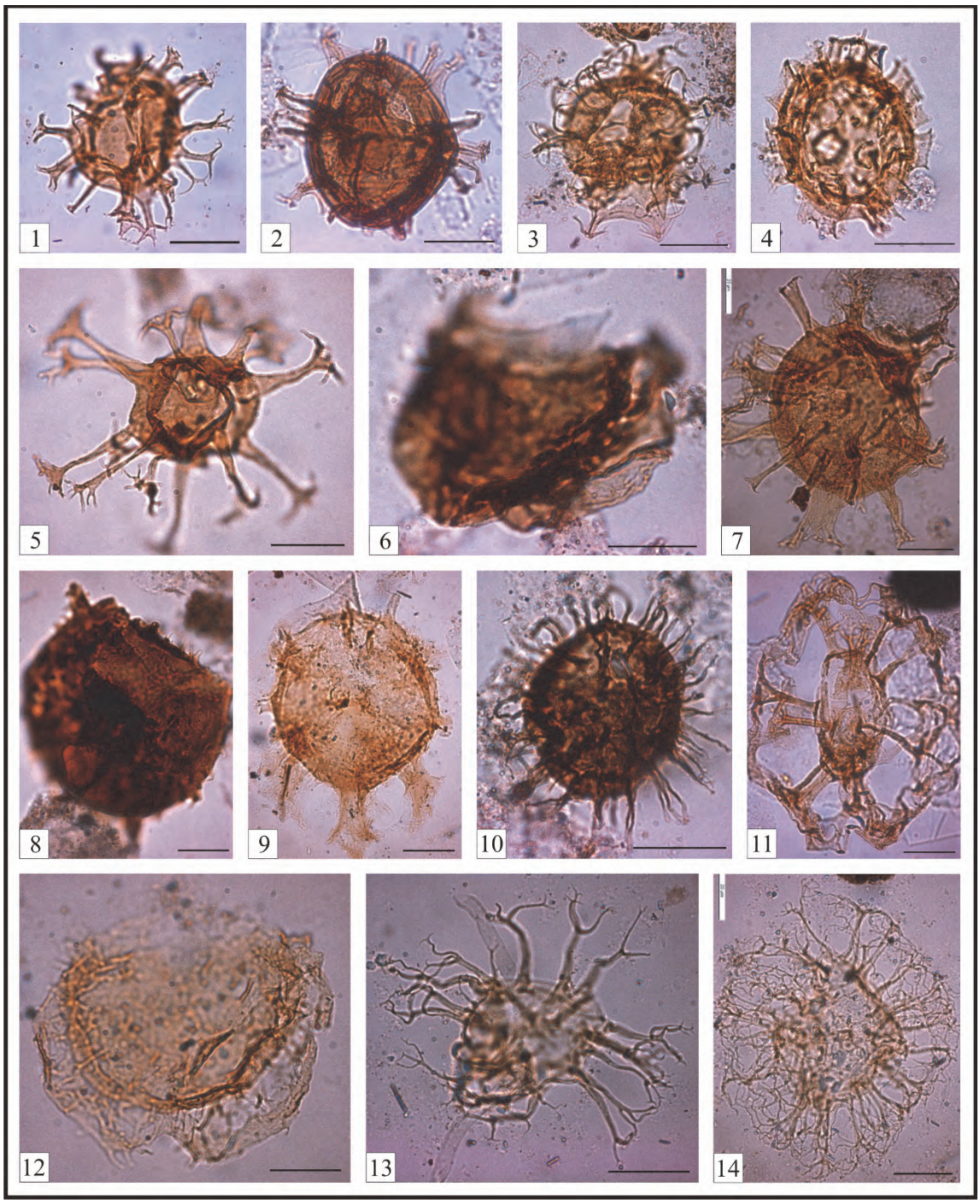

Fig. 27: Dinoflagellate taxa from the Goppling section (continuation). The species name is followed by sample location and England Finder coordinates (for localization of the specimen on the slide). Scale is 20 µm. 1) Achomosphaera cf. alcicornu - TS13/09/b, N5; 2) Spiniferites pseudofurcatus - TS4/09/b, X51/1; 3) Hystrichostrogylon membraniphorum - TS12/09/a, N24/2; 4) Achilleodinium biformoides - TS11/09/a, X8; 5) Oligosphaeridium complex - Ach. 2/09/a, G12; 6) Senoniasphaera inornata - Ach. 2/09/b, F40; 7) Cordosphaeridium fibrospinosum - TS12/09/a, B36/3; 8) Carpatella cornuta - Ach.1/09/b, K16; 9) Damassadinium californicum - TS11/09/a, P10; 10) Operculodinium centrocarpum - Ach.2/09/b, B25/4; 11) Rigaudella aemula - TS4/09/b, D18/1; 12) Glaphyrocysta perforate - TS11/09/a, S14/1; 13) Surculosphaeridium longifurcatum - TS11/09/a, M46/2; 14) Trabeculidium quinquetrum - TS12/09/a, D34/2.

Danian

Danian and Selandian deposits are almost continuously exposed in the Goppling creek gully. Due to the carbonate depletion, no calcareous plankton could be found in the siliciclastic succession, although dinoflagellate assemblages of samples Ach1/09 and Ach2/09 (see Fig. 27/6, 8 and 9) contain *Carpatella cornuta, Damassadinium californicum* and *Senoniasphaera inornata*, which have their first appearance date in the early Danian. *Palynodinium grallator* (Figs. 26/5 and 6) has its highest occurrence in the lowermost Danian planktonic foraminiferal Zone P1a (Habib et al., 1996; Dam et al., 1998; Brinkhuis et al., 1998). The samples were taken at the base (Ach1/09) and top (Ach2/09) of the same outcrop. Consequently, this outcrop can be assigned to Zone P1a in the zonation of Berggren et al. (1995).

The Danian shows a two-fold lithological subdivision. The 30 m thick lower part is dominated by thin-bedded (< 40 cm) parallel-laminated sandstone turbidites, that rarely show thin capping mudstone. In contrast to the Maastrichtian turbidites, the Danian ones are not calcite cemented and do not contain carbonate at all. They are fine-grained (grain diameters up to 0.2 mm), show clast supported fabrics, and have a quartzarenitic composition. Beside quartz (ca. 90 % of the grains), feldspar, chert and glauconite occur as components. Freimoser (1972) noted that the heavy mineral assemblages of these Paleocene sandstones are essentially composed of zircon, tourmaline and rutile (together about 90 % of the assemblage). Hemipelagic claystone between the turbidite beds is rare and when present only a few millimeters thick indicating that (1) turbidity currents entered the basin with a high frequency and (2) deposition took place below the local CCD.

In the 40 m thick upper part of the Danian, hemipelagic layers are common and often display red colors. Packages of red hemipelagic claystone contain thin base truncated turbiditic siltstone to sandstone beds. These packages are separated by single thick (>0.5 m) medium to coarse-grained sandstone beds showing grain diameters up to 1.0 mm. As in the lower Danian, only K-feldspar components can be observed and plagioclase is entirely absent. The beds are either massive or show stratification defined by 2-5 cm thick laminae. Graded (Ta) and parallel laminated (Tb) Bouma divisions form the major parts of these beds. Small-sized terrestrial plant remnants are commonly concentrated in horizontal Td-layers near the top of the beds and indicate a derivation of the turbidite material from land areas. Submarine erosion is evidenced by flute casts, which indicate sediment transport predominantly from the west, parallel to the approximately east-west trending slope.

One sample (Ach3/09) of the red claystone was studied for dinoflagellates but contained only *Areoligera senonensis*, which has a range from the Cretaceous to the Paleogene. Together with the last red hemipelagites, grey turbiditic clayey marlstones occur, containing strongly corroded nannoplankton assemblages. Beside substantial admixtures of Cretaceous species, *Chiasmolithus danicus, Cruciplacolithus tenuis, Coccolithus pelagicus* and *Toweius* spp. are indicative for the Danian (*Chiasmolithus danicus* Zone, NP3). However, the absence of *Ellipsolithus macellus*, the zonal marker for Zone NP4, might only be a consequence of the poor preservation in this sample.

Selandian

About 10 m up-section from the above mentioned Danian sample, nannoplankton assemblages contain *Fasciculithus tympaniformis*, the zonal marker for the calcareous nannoplankton Zone NP5 of earliest Selandian age. With the disappearance of red hemipelagites the discrimination between turbiditic and non-turbiditic rocks becomes difficult. Single turbidites show a distinct pelitic component (Bouma Td) in this part of the Goppling section, with approximately the same thickness as the sandy

part of the turbidite. This turbiditic mudstone only occasionally contains carbonate. In most cases it is devoid of carbonate and displays the same grey color as the supposed hemipelagic mudstone.

The Selandian, which forms the morphologically steepest part in the course of creek 3, is composed of a ca. 25 m thick thickening and coarsening upward succession. In the lower part of this succession decimeter-scale turbidites occur. Continuing up the exposure, the bed thicknesses gradually increase up to 1.5 m at the top of the succession. These sandstone beds are the thickest beds in the entire Achthal Formation and do not display turbiditic mudstone. In part, they contain intraformational mudstone clasts with diameters up to 0.2 m. Flute casts indicate paleotransport from west to east and thus an orientation parallel to the trend of the paleoslope.

Thanetian

In spite of excellent exposures along creek 3, the boundary between the Selandian and Thanetian is difficult to fix precisely due to carbonate depletion and the lack of calcareous plankton. Ca. 20 m downstream from the confluence in the uppermost part of creek 3 (Fig. 23), *Fasciculithus billii* is indicative for the upper part of Zone NP5. From here on upstream, a ca. 40 m thick part of the section is characterized by abundant olive-green strongly bioturbated „spotty“ claystone. Probably, the majority of the oval spots in these hemipelagic deposits represent cross sections of the trace fossils *Planolites* and *Thalassinoides* (Uchman, 1999). *Thalassinoides* ispp. and a strongly fragmented specimen of *?Scolica strozzii* were found also as semi-reliefs at the base of turbidite beds (Fig. 28/4, 28/5 and 28/6).

The turbidites intervening with the claystone are mostly thin bedded and occasionally display substantial amounts of glauconite, resulting in green rock colors. Glauconite was deformed during burial and flowed around adjacent quartz grains. This is indicated by the patchy distribution of glauconite-filled areas, which are much larger than normal pores.

Some beds show a lenticular shape. The orientation of paleoflow indicators (flute casts and erosional channels) suggest paleotransport from north to south, following the gradient of the south-facing paleoslope. *Discoaster mohleri* (Fig. 25/12) indicative of Thanetian zone NP7, was found in the eastern branch of creek 3, about 50 m up-stream from the confluence with the western branch (Fig. 23). *Discoaster multiradiatus* (Fig. 25/11), the zonal marker of Zone NP9, was found in the uppermost part of the western branch.

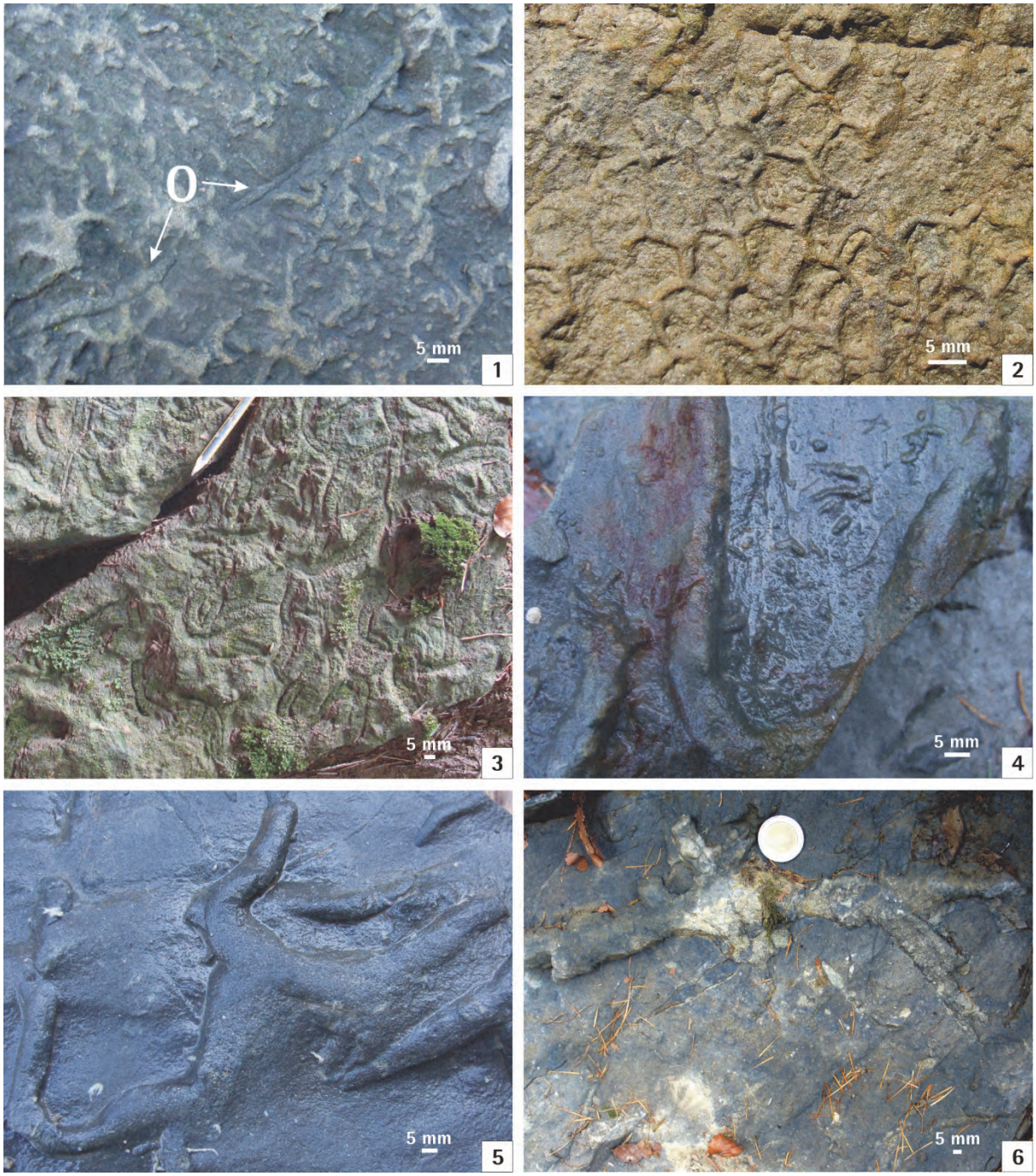

Fig. 28: Ichnofossils from the Thanetian (creek 3) and Ypresian (creek 4) of the Goppling section 1) Ophiomorpha annulata (O) and ? Protopaleodictyon isp. – creek 3; 2) Paleodictyon majus.- creek 4; 3) Scolicia prisca – creek 4; 4) ?Scolicia strozzii – creek 3; 5) Thalassinoides isp. – creek 3; 6) Thalassinoides isp. – creek 3.

Ypresian

The Ypresian of the Goppling section shows a two-fold lithological subdivision. The lower part consists of a ca. 50 m thick succession of decimeter-scale turbiditic sandstone and siltstone beds alternating with red colored marly claystone. The latter rock is often bioturbated and probably represents hemipelagic non-turbiditic material. As its carbonate values range between 4 wt% and 8 wt%, sedimentation slightly above the CCD can be assumed.

Samples containing *Rhomboaster cuspis* (Fig. 25/6 and 7) were found in the lower part of creek 5, about 20 m to the north of the hiking trail. *R. cuspis* has its first appearance date at the Paleocene/Eocene-boundary, which is situated in the upper third of Zone NP9. About 25 m to the south of the hiking trail, *Tribrachiatus digitalis* (Fig. 25/2) occurs, the marker fossil of sub-Zone NP10b in the refined zonation scheme of Aubry (1992). About 15 m further up-section, another outcrop of the red bed facies occurs and provided *Tribrachiatus orthostylus* (Fig. 25/1), whereas *T. contortus*, which has its highest occurrence at the NP10/NP11-boundary is absent. Therefore these samples can be assigned to the lower part of NP11 (*Discoaster binodosus*-Zone). Thus, in summary, the red bed facies encompasses the upper part of NP9 to the lower part of NP11.

Along strike to west, red beds containing *R. cuspis* were found in the upper part of creek 4. These deposits are separated by a fault from the underlying part of the succession in creek 4. In this gully, the topographically lowest outcrops lie just down-stream the hiking trail. *T. orthostylus* with pointed rays (Fig. 25/1) co-occurs with *Chiasmolithus bidens, Coccolithus pelagicus, Discoaster barbadiensis, D. multiradiatus, Ellipsolithus macellus* and *Sphenolithus primus*. Whereas the robust and dissolution resistant *Tribrachiatus* specimens may be common in the samples, the other species, in particular the discoasterids, are exceedingly rare due to dissolution. Carbonate values of two samples from this outcrop were 4.2 wt% and 4.8 wt%.

A few meters up-stream from the hiking trail the red bed facies in creek 4 shows a sharp sedimentary contact to an overlying ca. 60 m thick sand-rich and thin-bedded turbidite succession that displays only rare and very thin carbonate depleted hemipelagic layers. This suggests that the upper part of the Ypresian succession was deposited below the CCD and hence another subsidence pulse can be assumed. This interpretation is supported by the orientation of flute casts, which indicate paleoflow directions from west to east.

This part of the Goppling section commonly contains trace fossils (e.g. *Paleodictyon majus* and *Scolicia prisca*, see Fig. 28/2 and 3). According to Uchman (1999) the ichnogenus *Paleodictyon* probably reflects a moderate shortage of food. These generally oligotrophic conditions were interrupted by periodic accumulation of organic detritus (e.g. plant detritus) by turbidity currents. These more eutrophic episodes favored the ichnogenera *Ophiomorpha* and *Scolicia*. In the Rhenodanubian Group (Egger and Schwerd, 2008) of the adjacent abyssal Penninic basin, the ichnogenera *Ophiomorpha, Paleodictyon* and *Scolicia* are known exclusively from the Greifenstein Formation of Eocene age (Uchman, 1999).

Depositional evolution

Due to the lack of information about the three-dimensional geometry of the basin-fill, the scale and shape of this basin is unknown. It can be assumed that it was a narrow elongate, structurally controlled depression where tectonic activity was the primary control on sedimentation. Presumably, this confined basin was too small for the development of a large-scale deep-sea fan. Instead a channelized deep-water system could be expected, with the bounding slopes of the basin acting as channel walls

(Fig. 29). Gravity-induced flows entering a sub-basin drop their sediment load and prograde across the depression forming a thickening and coarsening upward succession (Anderson et al., 2006; Shultz and Hubbard, 2005).

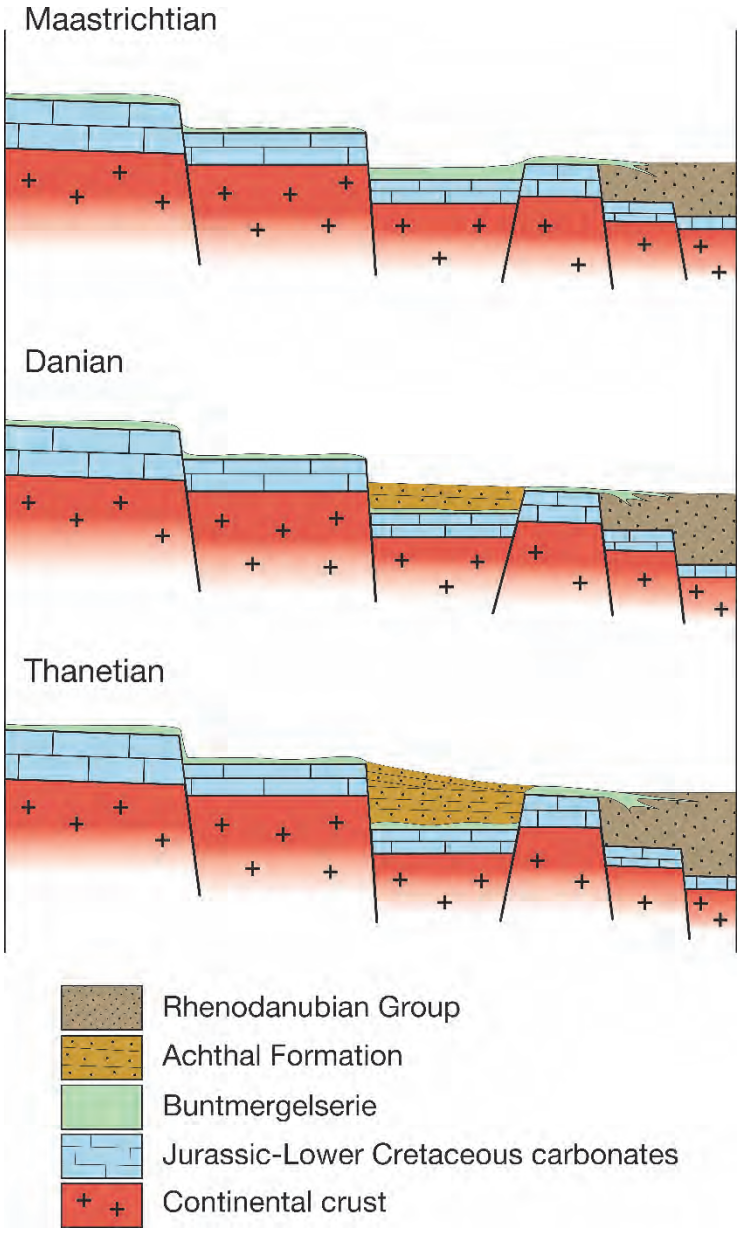

Fig. 29: Slope basin model for the deposition of the Achthal Formation.

At the front of this prograding lobe-like body the thin-bedded sand-rich turbidite succession of early Danian age was deposited (e.g. Crabaugh and Steel, 2004). The lack of muddy tops can be interpreted as an effect of flow-stripping of the fine-grained component of the turbidity currents (e.g. Piper and Normark, 1983; Sinclair and Tomasso, 2002). This indicates that during this early stage of basin evolution, the confining sill was still low. Hence it could be surmounted by the lower-density fraction of the turbidity currents, while the coarse-grained higher density portions of the flows were deflected and preserved upstream of the barrier. The rare and thin hemipelagites indicate the existence of high-

frequency trigger mechanisms (e.g. earthquakes) for turbidity currents during the onset of basin formation.

In a conventional fan model, the upper Danian packages of thin-bedded turbidites and red hemipelagic mudstone, which are separated by single thick sandstone beds, can be interpreted as interchannel deposits. In such a model, the thin-bedded turbidites are thought to result from low-density currents overflowing adjacent active channels, while the thicker beds are explained as the result of crevasses in the channel levee, which let high density turbidity currents (Lowe, 1982) escape to the basin floor (e.g. Mutti, 1977). This model implies the existence of subordinate fairways within the slope-basin.

Alternatively, the upper Danian facies can be seen as the result of an episode of comparatively tectonic quiescence. Siliciclastic material accumulated at the shelf edge over time and larger turbidity currents triggered by earthquakes or gravity load entered the slope-basin with low periodicity. This is indicated by the common occurrence of intervening hemipelagic red claystone as their deposition indicates very low sedimentation rates. The lack of muddy tops of the thick-bedded turbidites can again be explained as a result of flow-stripping as flow thickness was determined as the primary control of the run-up distance of a turbidity current onto the opposing slope (Muck and Underwood, 1990). It is assumed, that high-density currents (Lowe, 1982) lost their fine-grained component by down-spill, so that only their coarse-grained material is preserved in the sub-basin. Low-density currents had not the potential to surmount the bounding slope and remained completely in the sub-basin.

Increased subsidence at the end of the Danian caused ponding of the turbidity currents, which display a distinct pelitic component. However, sedimentation rates quickly outpaced subsidence rates and deposition reduced the relief sufficiently to allow spill down-slope. The filling up of the basin to the spill-point is indicated by downslope paleotransport directions in the upper Selandian and Thanetian. Due to the gradient reduction in the area of the former basinal structure turbidites were deposited on this flat surface and the ca. 95 m thick basin-fill succession of Danian and Selandian age became buried by slope deposits developing into a healed slope (e.g. Smith, 2004).

References

ANDERSON, K.S., GRAHAM, S.A. AND HUBBARD, S.M., 2006. Facies, architecture, and origin of a reservoir-scale sand-rich succession within submarine canyon fill: insights from Wagon Caves Rock (Paleocene), Santa Lucia Range, California, U.S.A. Journal of Sedimentary Research 76, 819–838.

AUBRY, M.-P., 1991. Sequence stratigraphy: Eustasy or tectonic imprint? Journal of Geophysical Research 96, 6641–6679.

AUBRY, M.-P., 1992. Towards an upper Paleocene - lower Eocene high resolution stratigraphy based on calcareous nannofossil stratigraphy. Israel Journal of Earth Sciences 44, 239–253.

BERGER, W.H., 1970. Planktonic foraminifera: selective solution and paleoclimatic interpretation. Marine Geology 8, 111–138.

BERGGREN, W.A., KENT, D.V., SWISHER, C.C. AND AUBRY, M.-P., 1995. A revised cenozoic geochronology and chronostratigraphy. Society for Sedimentary Geology Special Publication 54, 129–212.

BERGGREN, W.A. AND PEARSON, P.N., 2005. A revised tropical to subtropical Paleogene planktonic foraminiferal zonation. - Journal of Foraminiferal Research, 35, 279–298.

BØGGILD O.B., 1918. Den vulkanske Aske i Moleret samt en Oversigt over Danmarks ældre Tertiærbjærgarter. Danmarks Geologiske Undersøgelse (Series 2) 33, 1–159.

BOWEN, G.J., BRALOWER, T.J., DELANEY, M.L., DICKENS, G.R., KELLY, D.C., KOCH, P.L., KUMP, L.R., MENG, J., SLOAN, L.C., THOMAS, E., WING, S.L. AND ZACHOS, J.C., 2006. Eocene hyperthermal event offers insight into greenhouse warming. EOS 87, 165–169.

BRASS, G. W., SOUTHAM, J. R. AND PETERSON, W. H., 1982. Warm saline bottom water in the ancient ocean. Nature, 296, 620–623.

BRINKHUIS, H., 1994. Late Eocene to Early Oligocene dinoflagellate cysts from the Priabonian type-area (Northeast Italy): biostratigraphy and paleoenvironmental interpretation. – Palaeogeography, Palaeoclimatology, Palaeoecology, 107, 121–163.

BRINKHUIS, H., BUJAK, J.P., VERSTEEGH, G.J.M. AND VISSCHER, H., 1998. Dinoflagellate-based sea surface temperature reconstructions across the Cretaceous-Tertiary boundary. Palaeogeography, Palaeoclimatology, Palaeoecology 141, 67–83.

BRÜCKL, E., BEHM, M., DECKER, K., GRAD, M., GUTERCH, A., KELLER, G.R. AND THYBO, H., 2010. Crustal structure and active tectonics in the Eatern Alps. Tectonics 29, doi:10.1029/2009TC002491.

BUKRY, D., 1971. Cenozoic calcareous nannofossils from the Pacific ocean. Transactions San Diego Society of Natural History, 16, 303–328.

BUJAK, J.P., DOWNIE, C., EATON, G.L. AND WILLIAMS, G.L., 1980. Dinoflagellate cysts and acritarchs from the Eocene of Southern England. Special Papers in Palaeontology, 24, 3–100.

BUTT, A., 1981, Depositional environments of the Upper Cretaceous rocks in the northern part of the Eastern Alps: Cushman Foundation Foraminiferal Research, Special Publication, 20, 121 p.

BYBELL, L.M. AND SELF–TRAIL, J.M., 1994. Evolutionary, biostratigraphic, and taxonomic study of calcareous nannofossils from a continuous Paleocene–Eocene boundary section in New Jersey. U.S. Geological Survey Professional Papers, 1554, 1–107.

COLLINSON, M.E., 2000. Fruit and seed floras from the Palaeocene/Eocene transition and subsequent Eocene in southern England: Comparison and palaeoenvironmental implications. In: SCHMITZ, B., SUNDQUIST, B. AND ANDREASSON, F.P. (eds.). Early Paleogene Warm Climates and Biosphere Dynamics, GFF (Journal of the Geological Society of Sweden), 122, 36–37.

CRABAUGH, J.P. AND STEEL, R.J., 2004. Basin-floor fans of the Central Tertiary Basin, Spitsbergen: relationship of basin-floor sand-bodies to prograding clinoforms in a structural active basin. In: LOMAS, S.A. AND JOSEPH, P. (eds.): Confined turbidite systems. Geological Society, London, Special Publication 222, 187–208.

CROUCH, E. M., HEILMANN-CLAUSEN, C., BRINKHUIS, H., MORGANS, H.E.G., ROGERS, K.M., EGGER, H. AND SCHMITZ, B., 2001. Global dinoflagellate event associated with the Late Paleocene Thermal Maximum: Geology, 29, 315–318.

CROWELL, J.C., 1974. Origin of late Cenozoic basins in southern California. In: Dickinson, W.R. (ed.): Tectonics and Sedimentation. Society of Economic Paleontologists and Mineralogists Special Publication 22, 190–204.

DALE, B., 1996. Dinoflagellate cyst ecology: modelling and geological applications: In: JANSONIUS, J. AND MCGREGOR, D.C. (eds.), Palynology: principles and applications; American Association of Stratigraphic Palynologists Foundation, 3, 1249–1275.

DAM, G., NØHR-HANSEAN, H. AND KENNEDY, W. J., 1998. The northernmost marine Cretaceous-Tertiary boundary section: Nuussuaq, West Greenland. Geology of Greenland Survey Bulletin 180, 138–144.

DECKER, K. AND PERESSON, H., 1996. Tertiary kinematics in the Alpine-Carpathian-Pannonian system: links between thrusting, transform faulting and crustal extension. In: Wessely, G. and Liebl, W.: Oil and gas in Alpidic thrustbelts and basins of central and eastern Europe. – EAGE Special Publication, 5, 69–77.

DICKENS, G.R., 2000. "Methane oxidation during the late Palaeocene thermal maximum". Bulletin Société Géologique de France, 171, 37–49.

DRAXLER, I., 2007. Significant Palynomorphs from the Thanetian Kroisbach-Member in Salzburg (Eastern Alps, Austria). Jahrbuch der Geologischen Bundesanstalt, 357–377.

DYBKJÆR, K. AND RASMUSSEN, E.S., 2000. Palynological dating of the Oligocene – Miocene successions in the Lillebælt area, Denmark: Bulletin of the Geological Society of Denmark, 47, 87–103.

EATON, G.L., 1976. Dinoflagellate cysts from the Bracklesham Beds (Eocene) of the Isle of Wight, Southern England. Bulletin of the British Museum of Natural History and Geology, 26, 227–332.

EGGER, H., 1995. Die Lithostratigraphie der Altlengbach-Formation und der Anthering-Formation im Rhenodanubischen Flysch (Ostalpen, Penninikum). Neues Jahrbuch für Geologie und Paläontologie Abhandlungen 196, 69–91.

EGGER, H., BICHLER, M., HOMAYOUN, M. KIRCHNER, C. AND SURENIAN, R., 1995. Spätpaläozäne Bentonite aus der Gosau-Gruppe des Untersberg-Vorlandes (Nördliche Kalkalpen, Salzburg). Jahrbuch der Geologischen Bundesanstalt, 139, 13–20.

EGGER H., LOBITZER, H., POLESNY, H. AND WAGNER, L.R., 1997. Trip#1 – Cross section through the oil and gas-bearing Molasse basin into the alpine units in the area of Salzburg, Austria-Bavaria). Guidebook AAPG International Conference and Exhibition, 104p.

EGGER, H., HEILMANN-CLAUSEN, C. AND SCHMITZ, B., 2000. The Paleocene/Eocene-boundary interval of a Tethyan deep-sea section and its correlation with the North Sea Basin. Société Géologique de France Bulletin, 171, 207–216.

EGGER, H., HOMAYOUN, M. AND SCHNABEL, W., 2002. Tectonic and climatic control of Paleogene sedimentation in the Rhenodanubian Flysch Basin (Eastern Alps, Austria). Sedimentary Geology 152, 247–262.

EGGER, H., FENNER, J., HEILMANN-CLAUSEN, C., RÖGL, F. SACHSENHOFER, R.F. AND SCHMITZ, B., 2003. Paleoproductivity of the northwestern Tethyan margin (Anthering Section, Austria) across the Paleocene-Eocene transition. In: WING, S.L., GINGERICH, P., SCHMITZ, B., THOMAS, E. (eds.), Causes and Consequences of Globally Warm Climates in the Early Paleogene, Geological Society of America Special Paper, 369, 133–146.

EGGER, H., RÖGL, F. AND WAGREICH, M., 2004. Biostratigraphy and facies of Paleogene deep-water deposits at Gams (Gosau Group, Austria). Annalen Naturhistorisches Museum Wien, 106A, 281–307.

EGGER, H., HOMAYOUN, M., HUBER, H., RÖGL, F. AND SCHMITZ, B., 2005. Early Eocene climatic, volcanic, and biotic events in the northwestern Tethyan Untersberg section, Austria. Palaeogeography, Palaeoclimatology, Palaeoecology 217, 243–264.

EGGER, H. AND BRÜCKL, E., 2006. Gigantic volcanic eruptions and climatic change in the early Eocene. International Journal Earth Sciences, 95, 1065–1070.

EGGER, H. AND SCHWERD, K., 2008. Stratigraphy and sedimentation rates of Upper Cretaceous deep-water systems of the Rhenodanubian Group (Eastern Alps, Germany). Cretaceous Research 29, 405–416.

EGGER, H., HEILMANN-CLAUSEN, C. AND SCHMITZ, B., 2009. From shelf to abyss: Record of the Paleocene/Eocene-boundary in the Eastern Alps (Austria). Geologica Acta, 7, 215-227.

EGGER, H. AND MOHAMED, O., 2010. A slope-basin model for early Paleogene deep-water sedimentation (Achthal Formation nov. nom.) at the Tethyan continental margin (Ultrahelvetic realm) of the European Plate (Eastern Alps, Germany). Austrian Journal of Earth Sciences 103, 121–137.

EGGER, H., RÖGL, F., BIJL, P., BRINKHUIS, H. AND DARGA, R., 2011. The Middle Eocene transgression on the southern European shelf (Adelholzen beds, Eastern Alps, Bavaria. In: EGGER, H. (ed): Climate and Biota of the Early Paleogene, Conference Program and Abstracts, 5-8 June 2011, Salzburg, Austria. Berichte der Geologischen Bundesanstalt, 85, p.70.

ELDHOLM, O. AND GRUE, K., 1994. North-Atlantic Volcanic Margins: Dimensions and Production-Rates. Journal Geophysical Research, 99, 2955–2968.

FENNER, J., 1994. Diatoms of the Fur Formation, their taxonomy and biostratigraphic interpretation.– Results from the Harre borehole, Danmark: Aarhus Geoscience 1, 99–163.

FREIMOSER, M., 1972. Zur Stratigraphie, Sedimentpetrographie und Faziesentwicklung der Südostbayerischen Flyschzone und des Ultrahelvetikums zwischen Bergen / Obb. und Salzburg. Geologica Bavarica 66, 7–91.

FRISCH, W., 1979. Tectonic progradation and plate tectonic evolution of the Alps. Tectonophysics 60, 121–139

GEROCH, S. AND KAMINSKI, M. A., 1992. The morphology, palecology and systematics of Nothia excelsa (Grzybowski), a deep-water agglutinted foraminifer. Annales Societas Geologorum Poloniae, 62, 255–265.

GOODAY, A. J., SHIRES, R. AND JONES, A.R., 1997. Large, deep-sea agglutinated foraminifera: two different kinds of organization and their possible ecological significance. Journal of Foraminiferal Research, 27, 278–291.

GALEOTTI, S., ANGORI, E., COCCIONI, R., FERRARI, G., GALBRUN, B., MONECHI, S., PREMOLI-SILVA, I., SPEIJER, R. AND TURI, B., 2000. Integrated stratigraphy acros the Paleocene/Eocene boundary in the Contessa Road section, Gubbio (central Italy). Société Géologique de France Bulletin, 171, 355–366.

GANSS, O. AND KNIPSCHEER, H.C.G., 1956. Die Maastricht-Eozän-Folge des Helvetikums im Sprunggraben bei Oberteisendorf (Obb.) und ihre Gliederung mit Hilfe pelagischer Foraminiferen. Geologisches Jahrbuch 71, 617–630.

GOHRBANDT, K., 1963. Zur Gliederung des Paläogen im Helvetikum nördlich Salzburg nach planktonischen Foraminiferen. Mitteilungen der Geologischen Gesellschaft in Wien, 56, 1–116.

GRAUP, G. AND SPETTEL, B., 1989. Mineralogy and phasechemistry of an Ir-enriched pre-K/T layer from the Lattengebirge, Bavarian Alps, and significance for the KTB problem. Earth and Planetary Science Letters 95, 271–290.

GRACHEV, A.F., KORCHAGIN, O.A., KOLLMANN, H.A., PECHERSKY, D.M. AND TSELMOVICH, A., 2005. A new look at the nature of the transitional layer at the K/T boundary near Gams, Eastern Alps, Austria, and the problem of the mass extinction of the biota. Russian Journal of Earth Sciences, 7, 1–45.

GRACHEV, A.F., KORCHAGIN, O.A., TSELMOVICH, V.A. AND KOLLMANN, H.A., 2008. Cosmic dust and micrometeorites in the transitional clay layer at the Cretaceous-Paleogene boundary in the Gams Section. Physics of the Solid Earth, 44, 555–569.

GRACHEV, A.F., KAMENSKY, I.L., KORCHAGIN, O.A. AND KOLLMANN, H.A., 2007. The first data on helium isotopy in a transitional clay layer at the Cretaceous-Paleogene boundary (Gams, Eastern Alps). Physics of the Solid Earth, 43:766–772.

GRADSTEIN, F., OGG, J. AND SMITH, A., 2004. A Geologic Time Scale, 589 p. (Cambridge University Press).

GÜMBEL, C.W., 1862. Geognostische Beschreibung des bayerischen Alpengebirges und seines Vorlandes. 950 pp., Gotha (Justus Perthes).

HABIB, D., OLSSON, R.K., LIU, C. AND MOSHKOVITZ, S., 1996. High-resolution biostratigraphy of sea-level low, biotic extinction, and chaotic sedimentation of the Cretaceouse-Tertiary boundary in Alabama, north of the Chicxulub crater. In: RYDER, G., FASTOVSKY, D. AND GARTNER, S. (Eds.), The Cretaceous/Tertiary Event and Other Catastrophes in Earth history. Geological Society of America, Special Paper 307, 243–252.

HAGN, H., 1960. Die stratigraphischen, paläogeographischen und tektonischen Beziehungen zwischen Molasse und Helvetikum im östlichen Oberbayern. Geologica Bavarica 44, 5–208.

HAGN, H., 1967. Das Alttertiär der Bayerischen Alpen und ihres Vorlandes. Mitteilungen Bayerische Staatssammlung Paläontologie und historische Geologie 7, 245–320.

HAGN, H., 1981. Die Bayerischen Alpen und ihr Vorland in mikropaläontologischer Sicht (Exkursionsführer 17. Europäisches Mikropaläontologisches Kolloquium). Geologica Bavarica 82, 1–408.

HAGN, H., COSTA, L.I., HERM, D., HILLEBRANDT, A. V., HÖFLING, R., LINDENBERG, H.G., MALZ, H., MARTINI, E., MOUSSAVIAN, E., PERCH-NIELSEN, K., PFEIL, F.H., RISCH, H., SCHAUB, H., SCHMIDT, K., SCHROEDER, R., URLICHS, M., VOIGT, E., WEHNER, H., WEISS, W. AND WITT, W., 1981. Die Bayerischen Alpen und ihr Vorland in mikropaläontologischer Sicht (Exkursionsführer 17. europäisches Mikropaläontologisches Kolloquium. Geologica Bavaria 82, 1–408.

HAQ, B.U., HARDENBOL, J. AND VAIL, P.R., 1987. Mesozoic and Cenozoic Chronostratigraphy and eustatic cycles. Society of Economic Paleontologists and Mineralogists Special Publication 42, 71–108.

HARLAND, R., 1979. The Wetzeliella (Apectodinium) homomorpha plexus from the Paleogene/earliest Eocene of North-West Europe. IV International Palynological Conference, Lucknow (1976–1977), 2, 59–70.

HAY, W.W., 2004. Carbonate fluxes and calcareous nannoplankton. In: THIERSTEIN, H.R. AND YOUNG, J.R. (eds.): Coccolithophores, 509–528 (Springer).

HEILMANN-CLAUSEN, C., 1985. Dinoflagellate stratigraphy of the uppermost Danian to Ypresian in the Viborg 1 borehole, central Jylland, Denmark: Danmarks Geologiske Undersøgelse, ser. A, 7, 1–69.

HEILMANN-CLAUSEN, C. AND COSTA, L.I., 1989, Dinoflagellate Zonation of the Uppermost Paleocene? to Lower Miocene in the Wursterheide Research Well, NW Germany. Geologisches Jahrbuch, Ser. A, 111, 431–521.

HEILMANN-CLAUSEN, C., 1995. Palæogene aflejringer over Danskekalken. In: NIELSEN, O.B. (ed.). Danmarks geologi fra Kridt til i dag. Aarhus Geokompendier No. 1, 70–114.

HEILMANN-CLAUSEN, C. AND EGGER, H., 1997. An ash-bearing Paleocene/Eocene sequence at Anthering, Austria: biostratigraphical correlation with the North Sea Basin. Danmarks og Grønlands undersøgelse rapport, 1997/87, 13.

HEILMANN-CLAUSEN, C. AND EGGER, H., 2000. The Anthering outcrop (Austria), a key section for correlation between Tethys and northwestern Europe near the Paleocene/Eocene boundary: GFF (Journal of the Geological Society of Sweden), 122, 69.

HEILMANN-CLAUSEN, C. AND SCHMITZ, B., 2000. The late Paleocene thermal maximum $\delta^{13}C$ excursion in Denmark? – GFF (Journal of the Geological Society of Sweden), 122, p. 70.

HEILMANN-CLAUSEN, C. AND VAN SIMAEYS, S., 2005. Dinoflagellate cysts from the Middle Eocene to ?lowermost Oligocene succession in the Kysing research borehole, central Danish Basin. Palynology, 29, 141–204.

HEISTER, L.E., O´DAY, P.A., BROOKS, C.K., NEUHOFF, P.S. AND BIRD, D.K., 2001. Pyroclastic deposits within the East Greenland Tertiary flood basalts. Journal Geological Society London, 158, 269–284.

HERM, D., HILLEBRANDT, A. AND PERCH-NIELSEN, K., 1981. Die Kreide/Tertiärgrenze im Lattengebirge (Nördliche Kalkalpen) in mikropaläontologischer Sicht. Geologica Bavarica, 82, 319–344.

HESSE, R., 1975. Turbiditic and non-turbiditic mudstone of Cretaceous flysch sections of the East Alps and other basins. Sedimentology, 22, 387–416.

HESSE, R., 1982. Cretaceous-Paleogene Flysch Zone of the east Alps and Carpathians: identification and plate-tectonic significance of „dormant“ and „active“ deep-sea trenches in the Alpine-Carpathian Arc. In: LEGGETT, J.K. (Ed.). Trench-forearc geology. Geological Society of London Special Publication 10, 471–494.

HILLEBRANDT, A. V., 1962. Das Paleozän und seine Foraminiferenfaunen im Becken von Reichenhall und Salzburg. Bayerische Akademie der Wissenschaften mathematisch-naturwissenschaftliche Klasse Abhandlungen, 108, 1–113.

HILLEBRANDT, A. V., 1993. Nummuliten und Assilinen aus dem Eozän des Krappfeldes in Kärnten (Österreich). Zitteliana, 20, 277–293.

HOFMANN, CH.-CH., PANCOST, R., OTTNER, F., EGGER, H., TAYLOR, K., MOHAMED, O. AND ZETTER, R., 2011. Palynology, biomarker assemblages and clay mineralogy of the Early Eocene Climate Optimum (EECO) in the transgressive Krappfeld succession (Eastern Alps, Austria). Austrian Journal of Earth Sciences, 105/1, 224–239.

HUBER, H., KOEBERL, C. AND EGGER, H., 2003. Geochemical study of Lower Eocene volcanic ash layers from the Alpine Anthering Formation, Austria. Geochemical Journal, 37, 123–134.

IAKOVLEVA, A.I. AND HEILMANN-CLAUSEN, C., 2007. Wilsonidium pechoricum new species – a new dinoflagellate species with unusual asymmetry from the Paleocene/Eocene transition. J. Paleont.8, 1020–1030.

JONES, R.W. AND CHARNOCK, M.A., 1985, „Morphogroups“ of agglutinating foraminifera. Their life positions and feeding habits and potential applicability in (paleo)ecological studies. Revue Paleobiologique, 4, 311–320.

KAMINSKI, M.A., GRADSTEIN, F.M. AND BERGGREN, W.A., 1989. Palaeogene benthic foraminifer biostratigraphy and Palaeoecology at Site 647, southern Labrador Sea. In: SRIVSTAVA, S.P., ARTHUR, M.A. AND CLEMENT, B. et al., Proceedings of the Ocean Drilling Program, Scientific Results, 105, 705–730.

KAMINSKI, M.A., KUHNT, W. AND RADLEY, J.D., 1996. Palaeocene–Eocene deep water agglutinated foraminifera from the Numidian Flysch (Rif, Northern Morocco): their significance for the palaeoceanography of the Gibraltar gateway. Journal of Micropalaeontology, 15, 1–19.

KAMINSKI, M.A., KUHNT, W. AND MOULLADE, M., 1999. The evolution and paleobiogeography of abyssal foraminifera since the Early Cretaceous: a tale of four faunas: Neues Jahrbuch Geologie Paläontologie Abhandlungen, 212, 401–439

KEDVES, M., 1980. Palynological investigations on Austrian Upper Cretaceous and Lower Tertiary sediments. Acta Biologica Szeged, 26, 63–77.

KLEY, J. AND VOIGT, T., 2008. Late Cretaceous intraplate thrusting in central Europe: Effect of Africa-Iberia-Europe convergence, not Alpine collision. Geology 36, 839–842.

KNELLER, B. AND MCCAFFREY, W., 1999. Depositional effects of flow nonuniformity and stratification within turbidity currents approaching a bounding slope: deflection, reflection and facies variation. Journal of Sedimentary Research 69, 980–991.

KÖTHE, A., 1990. Paleogene Dinoflagellates from Northwest Germany. Geologisches Jahrbuch, Serie A, 118, 3–111.

KNOX, R.W.O'B , 1984. Nannoplankton zonation and the Paleocene/Eocene boundary beds of northwestern Europe: An indirect correlation by means of volcanic ash layers. Journal Geological Society London 141:993–999.

KNOX, R.W.O'B. AND MORTON, A. C., 1988. The record of early Tertiary North Atlantic volcanism in sediments from the North Sea Basin. Early Tertiary Volcanism and the Opening of the NE Atlantic (MORTON, A. C. AND PARSON, L. M., eds.), Geological Society London Special Publication, 39, 407–419.

KNOX, R.W.O'B., 1998. The Tectonic and Volcanic History of the North Atlantic Region During the Paleocene-Eocene Transition: Implications for the NW European and Global Biotic Events. In: AUBRY, M.-P., LUCAS, S. AND BERGGREN, W.A. (Eds.), Late Paleocene-Early Eocene Climatic and Biotic Events in the Marine and Terrestrial Records, Columbia University Press, New York, 91–102.

KUHN, W. AND WEIDICH, K.F., 1987. Neue mikropaläontologische Ergebnisse aus dem Paleozän des Haunsberg-Helvetikums (Salzburg, Österreich). Paläont. Zeitschrift 61, 181–201.

KUHNT, W., KAMINSKI, M.A. AND MOULLADE, M., 1989. Late Cretaceous deep-water agglutinated foraminiferal assemblages from the North Atlantic and its marginal seas. Geologische Rundschau, 78, 1121–1140.

LAHODYNSKY, R., 1988. Lithostratigraphy and sedimentology across the Cretaceous/Tertiary Boundary in the Flyschgosau (Eastern, Alps, Austria). – Revista Espanola Paleontologia Special Volume, 1988, 73–82.

LARSEN, L.M., FITTON, J.G. AND PEDERSEN, A.K., 2003. Paleogene volcanic ash layers in the Danish Basin: compositions and source areas in the North Atlantic Igneous Province. Lithos, 71, 47–80.

LOWE, D.R., 1982. Sediment gravity flows: II. Depositional models with special reference to the deposits of high-density turbidity currents. Journal of Sedimentary Petrology 52, 279–297.

LUTERBACHER, H. P., ALI, J. R., BRINKHUIS, H., GRADSTEIN, F.M., HOOKER, J.J., MONECHI, S., OGG, J.G., POWELL, J., RÖHL, U., SANFILIPPO, A. AND SCHMITZ, B., 2004. The Paleogene Period. In: GRADSTEIN, F.M., OGG, J.G. AND SMITH, A.G., (eds.). A Geologic Time Scale 2004. Cambridge University Press, 384–408.

MENKVELD-GFELLNER, U., 1997. Die Bürgen-Fm. Und die Klimsenhorn-Fm.: Formelle Definition zweier lithostratigraphischer Einheiten des Eozäns der helvetischen Decken. Eclogae geol. Helv. 90, 245–261.

MUCK, M.T. AND UNDERWOOD, M.B., 1990. Upslope flow of turbidity currents: A comparison among field observations, theory, and laboratory models. Geology 18, 54–57.

MUTTI, E., 1977. Distinctive thin-bedded turbidite facies and related depositional environments in the Eocene Hecho Group (South-central Pyrenees, Spain). Sedimentology 24, 107–131.

NACHTMANN, W. AND WAGNER, L., 1987. Mesozoic and early Tertiary evolution of the Alpine foreland in Upper Austria and Salzburg, Austria. Tectonophysics 137, 61–76.

NEUBAUER, F., GENSER, J. AND HANDLER, R., 2000. The Eastern Alps: Result of a two-stage collision process. Mitteilungen österreichische geologische Gesellschaft, 92, 117–134.

NICOLO, M.J., 2008. Multiple early Eocene hyperthermal events: Their lithologic expressions and environmental consequences. Unpublished PhD Thesis, Rice University (http://scholarship.rice.edu/handle/1911/26797).

OBERHAUSER, R., 1991. Erläuterungen zur geologischen Karte der Republik Österreich 1: 25.000 Blatt 110 St. Gallen Süd und 111 Dornbirn Süd. 72 pp., Vienna (Geologische Bundesanstalt).

PERCH-NIELSEN, K., MCKENZIE, J. AND HE, Q., 1982. Biostratigraphy and isotope stratigraphy and the „catastrophic" extinction of calcareous nannoplankton at the Cretaceous/Tertiary boundary.- In: SILVER, L.T. AND SCHULTZ, P.H. (eds.): Geological Implications of Impacts of Large Asteroids and Comets on the Earth. Geological Society of America Special Paper, 190, 353–371.

PERYT, D., LAHODYNSKY, R., ROCCHIA, R. AND BOCLET, D., 1993. The Cretaceous/Paleogene boundary and planktonic foraminifera in the Flyschgosau (Eastern Alps, Austria). Palaeogeography, Palaeoclimatology, Palaeoecology, 104, 239–252.

PERYT, D., LAHODYNSKY, R. AND DURAKIEWICZ, T., 1997. Deep-water agglutinated foraminiferal changes and stable isotope profiles across the Cretaceous-Paleogene boundary in the Rotwand section, Eastern Alps (Austria). Palaeogeography, Palaeoclimatology, Palaeoecology, 132, 287–307.

PIPER, D.J.W. AND NORMARK, W.R., 1983.Turbidite-deposits, patterns and flow characteristics, Navy Submarine Fan, California borderland. Sedimentology 30, 681–694.

PREISINGER, A., ZOBETZ, E., GRATZ, A., LAHODYNSKY, R., BECKE, M., MAURITSCH, H.J., EDER, G., GRASS, F., RÖGL, F., STRADNER, H. AND SURENIAN, R., 1986. The Cretaceous/Tertiary boundary in the Gosau Basin, Austria. Nature, 322, 797–799.

PREY, S., 1952. Aufnahmen in der Flyschzone auf den Blättern Gmunden-Schafberg (4851) und Kirchdorf/Krems (4852) (Gschliefgraben), sowie den Blättern Ybbs (4754) und Gaming-Mariazell (4854) (Rogatsboden). – Verhandlungen der Geologischen Bundesanstalt 1952, 41–45.

PREY, S., 1957. Ergebnisse der bisherigen Forschungen über das Molassefenster von Rogatsboden (NÖ.). Jahrbuch der Geologischen Bundesanstalt 100, 299–358.

PUJALTE, V. AND SCHMITZ, B., 2006. Abrupt climatic and sea level changes across the Paleocene-Eocene boundary, as recorded in an ancient coastal plain setting (Pyrenees, Spain). Climate and biota of the Early Paleogene Abstracts, p. 103 (Bilbao).

RASSER, M.W. AND PILLER, W.E., 1999. Kroisbachgraben und Frauengrube: Lithostratigraphische Typuslokalitäten für das paläogene Helvetikum in Salzburg. Abhandlugen Geologische Bundesanstalt, 56, 713–722.

RASSER, M.W. AND PILLER, W.E., 2001. Facies patterns, subsidence and sea-level changes in ferriginous and glauconitic environments: The Paleogene Helvetic shelf in Austria and Bavaria. Österreichische Akademie der Wissenschaften Schriftenreihe der Erdwissenschaftlichen Kommissionen, 14, 77–110.

RITCHIE, J. D. AND HITCHEN, K., 1996. Early Paleogene offshore igneous activity to the northwest of the UK and its relationship to the North Atlantic igneous province. Correlation of the Early Paleogene in Northwest Europe (KNOX, R. W. O'B., CORFIELD, R. M. AND DUNAY, R. E., eds.), Geological Society London Special Publication, 101, 63–78.

RODRÍGUEZ-TOVAR, F.J., UCHMAN, A., ALEGRET, L. AND MOLINA, E., 2011. Impact of the Paleocene-Eocene Thermal Maximum on the macrobenthic community: ichnological record from the Zumaia section, northern Spain. Marine Geology, 282, 178–187.

RÖGL, F. AND EGGER, H., 2010. The missing link in the evolutionary origin of the foraminiferal genus Hantkenina and the problem of the lower-middle Eocene boundary. Geology 38, 23–26.

RÖHL, U., BRALOWER, T.J., NORRIS, R.D. AND WEFER, G., 2000. New chronology for the late Palaeocene thermal maximum and its environmental implications. Geology, 28, 927–930.

ROSS, P.S., UKSTINS, A., PEATE, I., MCCLINTOCK, M.K., XU, Y.G., SKILLING, I.P., WHITE, J.D.L. AND HOUGHTON, B.F., 2005. Mafic volcaniclastic deposits in flood basalt provinces: A review. Journal Volcanology Geothermal Research, 145, 281–314.

SCHAFHÄUTL, K., 1846. Beiträge zur näheren Kenntnis der Bayerischen Voralpen. Neues Jahrbuch für Mineralogie, Geognosie, Geologie und Petrefaktenkunde 1846, 641–695 (Stuttgart).

SCHAUB, H., 1981. Nummulites et Assilines de la tethys paleogene, taxonomie, phylogenese et biostratigraphie. Memoires Suisses de Paleontologie 104, 1–236.

SCHLOSSER, M., 1925. Die Eocänfaunen der bayerischen Alpen. 1. Teil: Die Faunen des Unter- und Mitteleocaen. Abhandlungen Bayerische Akademie der Wissenschaften, Mathematisch-naturwissenschaftliche Abteilung, 30, 1–207.

SCHMITZ, B., PUJALTE, V. AND NUNEZ-BETELU, K., 2001. Climate and sea–level perturbations during the Initial Eocene Thermal Maximum: evidence from siliciclastic units in the Basque Basin (Ermua, Zumaia and Trabakua Pass), northern Spain. Palaeogeography, Palaeoclimatology, Palaeoecology, 165, 299–320.

SCHMITZ, B. AND PUJALTE, V., 2007. Abrupt increase in extreme seasonal precipitation at the Paleocene-Eocene boundary. Geology, 35, 215–218.

SCHWERD, K., 1996. Ultrahelvetikum. In: Freudenberger, W. and Schwerd, K.: Erläuterungen zur Geologischen Karte von Bayern 1:500 000, 205–210.

SCHWERD, K. AND RISCH, H., 1983. Zur Stratigraphie und Herkunft der Feuerstätter Decke im Oberallgäu. Jahresberichte Mitteilungen der oberrheinischen geologischen Vereinigung Neue Folge 65, 279–290.

SERRA-KIEL, J., HOTTINGER, L., CAUS, E., DROBNE, K., FERRANDEZ, C., JAURHI, A.K., LESS, G., PAVLOVEC, R., PIGNATTI, J., SAMSO, J.M., SCHAUB, H., SIREL, E., STROUGO, A., TAMBAREAU, Y., TOSQUELLA, J. AND ZAKREVSKAYA, E., 1998. Larger foraminiferal biostratigraphy of the Tethyan Paleocene and Eocene. Société Géologique de France Bulletin, 169, 281–299.

SHULTZ, M.R. AND HUBBARD, S.M., 2005. Sedimentology, stratigraphic architecture, and ichnology of gravity-flow deposits partially ponded in a growth-fault-controlled slope minibasin, Tres Pasos Formation (Cretaceous). Journal of Sedimentary Research 75, 440–453.

SINCLAIR, H.D. AND TOMASSO, M., 2002. Depositional evolution of confined turbidite basins. Journal of Sedimentary Research 72, 451–456.

SMITH, R., 2004. Silled sub-basins to connected tortuous corridors: sediment distribution systems on topographically complex sub-aqueous slopes. In: LOMAS, S.A. AND JOSEPH, P. (Eds.): Confined Turbidite Systems. Geological Society London Special Publication 222, 23–43.

STAMPFLI, G.M., MOSAR, J., MARQUER, D., MARCHANT, R., BAUDIN, T. AND BOREL, G., 1998. Subduction and obduction processes in the Swiss Alps. Tectonophysics, 296, 159–204.

STAMPFLI, G.M., BOREL, G., MARCHANT, R. AND MOSAR, J., 2002. Western Alps geological constraintson western Tethyan reconstructions. Journal virtual explorer 8, 77–106.

STEINMETZ, J.C., 1979. Calcareous nannofossils from the North Atlantic ocean, Leg 49, Deep Sea Drilling Project. Initial Reports of the Deep Sea Drilling Project, 49, 519–531.

STEURBAUT, E., MAGIONCALDA, R., DUPUIS, C., VAN SIMAEYS, S., ROCHE, E. AND ROCHE, M., 2003. Palynology, paleoenvironments, and organic carbon isotope evolution in lagoonal Paleocene–Eocene boundary settings in North Belgium. In: WING, S.L., GINGERICH, P., SCHMITZ, B., THOMAS, E. (eds.), Causes and Consequences of Globally Warm Climates in the Early Paleogene, Geological Society of America Special Paper, 369, 291–317.

STOVER, L.E., BRINKHUIS, H., DAMASSA, S.P., DE VERTEUIL, L., HELBY, R.J., MONTEIL, E., ARTRIDGE, A.D., POWELL, A.J., RIDING, J.B., SMELROR, M. AND WILLIAMS, G.L., 1996. Mesozoic-Tertiary dinoflagellates, acritarchs and prasinophytes. In: JANSONIUS, J. AND MCGREGOR, D.C. (Eds.), Palynology: principles and applications. American Association of Stratigraphic Palynologists Foundation, Dallas 2, 641–750.

STRADNER, H., EDER, G., GRASS, F., LAHODYNSKY, R., MAURITSCH, H.J., PREISINGER, A., RÖGL, F., SURENIAN, R., ZEISSL, W. AND ZOBETZ, E., 1987. New K/T boundary sites in the Gosau Formation of Austria. Terra cognita, 7, 212 (Paris).

THIRY, M., 2000. Palaeoclimatic interpretation of clay minerals in marine deposits: an outlook from the continental origin. Earth Science Reviews 49, 201–221.

UCHMAN, A., 1999. Ichnology of the Rhenodanubian Flysch (Lower Cretaceous-Eocene) in Austria and Germany. Beringeria 25, 67–173.

VAN MORKHOVEN, F.P.C.M., BERGGREN, W.A. AND EDWARDS, A.S., 1986. Cenozoic cosmopolitan deep-water benthic foraminifera. Bulletin Centres Recherches Exploration-Production Elf-Aquitaine Memoir 11, 1–421.

VOGELTANZ, R., 1977. Geologie des Wartstein-Straßentunnels, Umfahrung Mattsee (Land Salzburg). Verhandlungen der Geologischen Bundesanstalt, Jahrgang 1977, 279–291.

WADE, B. S., PEARSON, P.N., BERGGREN, W.A. AND PÄLIKE, H., 2011. Review and revision of Cenozoic tropical planktonic foraminiferal biostratigraphy and calibration to the geomagnetic polarity and astronomical time scale. Earth-Science Reviews 104, 111–142.

WAGREICH, M., 1993. Subcrustal tectonic erosion in orogenic belts – A model for the Late Cretaceous subsidence of the Northern Calcareous Alps (Austria). Geology, 21, 941–944.

WAGREICH, M., EGGER, H., GEBHARDT, H., MOHAMED, O., SPÖTL, C., KOUKAL, V. AND HOBIGER, G., 2011. A new expanded record of the Paleocene-Eocene transition in the Gosau Group of Gams (Eastern Alps, Austria). Annalen Naturhistorisches Museum Wien, A113, 35–65.

WAŚKOWSKA-OLIWA, A. AND LEŚNIAK, T., 2002. Lower Eocene tuffites in the Żegocina Zone (Polish Flysch Carpathians). Geologica Carpathica, 53, 45–47.

WEIDICH, K.F. AND SCHWERD, K., 1987. Über den Feuerstätter Flysch im Allgäu. Neues Jahrbuch für Geologie und Paläontologie Abhandlungen 174, 193–212.

WESSELY, G., 1987. Mesozoic and Tertiary evolution of the Alpine-Carpathian foreland in eastern Austria. Tectonophysics 137, 45–59.

WINCHESTER, J.A. AND FLOYD, P.A., 1977. Geochemical discrimination of different magma series and their differentiation products using immobile elements. Chemical Geology, 20, 325–343.

WINKLER W., GALETTI G. AND MAGGETTI, M., 1985. Bentonite im Gurnigel–, Schlieren- und Wägital–Flysch: Mineralogie, Chemismus, Herkunft. Eclogae Geologica Helvetiae, 78, 545–564.

ZACHOS, J.C., RÖHL, U., SCHELLENBERG, S.A., SLUIJS, A., HODELL, D.A., KELLY, D.C., THOMAS, E., NICOLO, M., RAFFI, I., LOURENS, L.J., MCCARREN, H. AND KROON, D., 2005. Rapid acidification of the ocean during the Paleocene-Eocene thermal maximum. Science 308, 1611–1615.

ZIEGLER, P.A., 1987. Late Cretaceous and Cenozoic intra-plate compressional deformations in the Alpine foreland – a geodynamic model. Tectonophysics 137, 389–420.

ZIEGLER, P.A., BERTOTTI, G. AND CLOETHING, S., 2002. Dynamic processes controlling foreland development – the role of mechanical (de)coupling of orogenic wedges and forelands. In. Bertotti, G. et al. (eds.): Continental collision and the tectono-sedimentary evolution of forelands. EGU Stephan Müller Special Publication Series 1, 17–56.